Evaluating Hydrologic, Geomorphic, and Vegetation Parameters to Assess Natural, Living, and Hardened Shorelines along the Northern Gulf of Mexico

Gabrielle Spellmann[1], Patrick Biber[1]

1 University of Southern Mississippi

Funding: No specific funding was received for this work.

Potential competing interests: No potential competing interests to declare.

Abstract

Living shorelines are a way of protecting the shoreline from erosion while supporting the productivity of coastal habitats to maintain their many desirable ecosystem services. We focused on evaluating hardened versus living shorelines for coastal protection and compared them to adjacent natural marsh shorelines suffering excess erosion rates. Living shorelines are a suite of shoreline conservation and restoration techniques, which usually involve a breakwater that dampens wave energy so vegetation can take root and stabilize the shoreline sediments. This synthesis looked at six different sites, all containing a natural, living, and hardened shoreline across two different energy groups (low and high) to see how hydrologic, geomorphic, and vegetative parameters affected shoreline processes. The erosion rate of the coastline and its geomorphic shape were significantly influenced in the two energy groups, with the high energy coastlines eroding more quickly and having a steeper slope. Hardened shorelines were found to have little to no erosion, while natural shorelines had the greatest amount of edge erosion over time. Living shorelines lessened this rate of erosion compared to the natural marsh. The natural and living shorelines were similar in slope and sediment parameters, while hardened shorelines had steep slopes and higher sand content. We found that coastlines with high turbidity, high erosion rates, large wave power, and relative exposure resulted in steeper slopes and a higher

percentage of sand in the sediment, but reduced vegetation percent cover and percent of marsh dominant vegetation species. This research increases our knowledge about what environmental conditions may be most suitable for living shorelines, of importance as sea levels rise and increase coastal erosion rates.

Gabrielle Spellmann[1,2] and **Patrick Biber**[1,2,*]

[1] *Division of Coastal Sciences, School of Ocean Science and Engineering, The University of Southern Mississippi*

[2] *Gulf Coast Research Laboratory, 703 East Beach Drive, Ocean Springs, Mississippi, U.S.A*

[*]Email: Patrick.biber@usm.edu

Introduction

There has been a decline in natural marshes worldwide because of coastal development, pollution, sea level rise, and other anthropogenic impacts (Sweet et al., 2017; IPCC, 2021). Sea level will continue to rise and endanger many coastlines (Sweet et al., 2017); this will cause properties to become flooded resulting in the loss of homes and other infrastructure (Temmerman et al., 2013). Human actions have already removed many coastal marshes; the resulting decline in vegetated habitat has further exacerbated coastal erosion (Gedan et al., 2011). Saltmarshes preserve coastal areas through increased sedimentation and storm protection, and the removal of these habitats has diminished their ecosystem services (Arkema et al., 2013) leading to more frequent flooding in many areas (Temmerman et al., 2013; Sutton-Grier et al., 2015). Property owners try to prevent flooding and erosion from occurring by armoring their shoreline with seawalls and bulkheads, which provide immediate protection to the property. While stopping erosion, armoring destroys the vegetated marsh ecosystem, and a better solution may be to use living shorelines that can mimic natural habitats and processes.

Natural Shorelines

There are many benefits provided by a healthy saltmarsh ecosystem (Craft et al., 2009; Bilkovic & Mitchell, 2018). Saltmarshes prevent erosion, clean the water, and create habitat and act as a transitional habitat between the sea and the land. Land protection is provided by the vegetation as it helps with wave energy reduction and storm surge dampening by decreasing the physical impact of waves that cause sediment erosion (Wu et al., 2012). Saltmarsh ecosystems also provide benefits for coastal waterways as the vegetation filters runoff and increases sediment retention. The filtration of runoff provided by saltmarshes makes the water more aesthetically pleasing and protects organisms and aquatic vegetation from nutrient loads that could be detrimental (Valiela & Cole, 2002; Álvarez-Rogel et al., 2016; Johnson et al., 2016). Saltmarshes are a source of both primary and secondary production (Bilkovic & Roggero, 2008), as they host salt-tolerant plant species that are an important source of organic matter (Craft et al., 2003; Currin et al., 2008; Matzke & Elsey-Quirk, 2018). Saltmarshes are an important habitat for many organisms because they provide both food and

protection from predators (Cattrijsse et al., 1997; Green et al., 2012; Sutton-Grier et al., 2015; Balouskus & Targett, 2016). Humans benefit from these many ecosystem services, such as shoreline stabilization, because it protects human development from flooding and destruction (Augustin et al., 2009; Arkema et al., 2013; Silliman et al., 2019).

Hardened Shorelines

As saltmarshes have declined, property owners have taken action to prevent coastal erosion by building hardened shorelines (Erdle et al., 2006; Swann, 2008; Gittman et al., 2016). Hardened shorelines include sea walls, jetties, revetments, breakwaters, and bulkheads. They provide immediate erosion protection, however, their many negative ecosystem consequences only become apparent over time. Hardened shorelines interrupt natural water flows and coastal morphodynamic processes, as well as sediment transportation by longshore currents. They can increase local erosion because of waves reflecting off the hardened structure (Bozek & Burdick, 2005; Ruggiero, 2009; Gittman et al., 2015), which causes increased sediment erosion and scouring at the base of the hardened structure (Basco, 2006; Roberts, 2010; Bilkovic & Mitchell, 2018). Coarser sediment, such as sand or gravel, builds up around the base of the hardened structure and results in a spatial gradient towards finer silt or clay sediments, with increased distance from the hardened structure (Bozek & Burdick, 2005; Palinkas et al., 2018). Sand is coarse, which makes it easier to be displaced by waves and currents (Bilkovic & Mitchell, 2013; Palinkas et al., 2018), however, sand grains are heavy and will quickly settle out of the water column (Molinaroli et al., 2009). More exposed sites with high wave energy tend to have more coarse and more dense sediment particles and contain less organic material (Bozek & Burdick, 2005). The increased sediment grain size nearshore can negatively affect vegetation, which reduces overall sedimentation (Craft et al., 2003; Vargas-Luna et al., 2015), potentially resulting in more turbid water conditions. Ecosystem services are interrupted due to the loss of vegetation and organisms after the implementation of a hardened structure (Roberts, 2010) in part driven by this change in sediment properties. The lack of intertidal vegetation at hardened shorelines has been documented to have subsequent negative effects on fish communities (Bilkovic & Roggero, 2008; Balouskus & Targett, 2016; Crum et al., 2018).

Living Shorelines

Living shorelines are an alternative method to combat erosion while also mitigating the numerous negative effects of hardened shorelines. They attempt to mimic natural coastal processes while still dissipating wave energy impacts along the shoreline (Erdle et al., 2006). Living shorelines are usually created by placing an intertidal hardened structure to act as a breakwater in front of planted marsh vegetation with the purpose of recreating ecosystem functioning like that of a natural marsh (Scyphers et al., 2011); but it can involve only planting, or addition of a breakwater structure without vegetation. The vegetation can take root as the breakwater structure provides erosion protection by reducing wave energy and erosion (Madsen et al., 2001; Swann, 2008). Living shorelines are a way of protecting the shoreline and maintaining the productivity of the ecosystem, thereby protecting many desirable ecosystem services (Swann, 2008; O'Donnell, 2017; Bilkovic & Mitchell, 2018) including erosion reduction, wave attenuation, habitat heterogeneity, and vegetation migration (Bilkovic et al., 2016). However, living shorelines will not immediately function like their natural marsh counterparts, because they must undergo vegetation and habitat succession (Boerema et al., 2016; Bilkovic & Mitchell, 2018). It takes a

number of years for primary producers to reach similar productivity and density as adjacent marshes; and sedimentary biogeochemical processes can take even longer, potentially a decade or more (Craft et al., 2003; Boerema et al., 2016). The vegetation at an established living shoreline plays a crucial role in enhancing sedimentation and low wave energy conditions (Brueske & Barrett, 1994; Feagin et al. 2009). Sedimentation increases in the presence of vegetation because it creates drag in the water flow (Madsen et al., 2001; Vargas-Luna et al., 2015). Marsh vegetation can affect wave dampening differently depending on stem density and flexibility (Fonseca & Cahalan, 1992; Augustin et al., 2009; Gedan et al., 2011). For instance, Wu et al. (2012) found that because *Sporobolus alterniflorus* (smooth cordgrass) has more leaves and dormant plant material than *Juncus roemerianus* (black needlerush), it has a higher drag coefficient meaning that it has a greater effect on reducing wave energy. Other research has found that plants prevent erosion as the roots bind the deposited sediments together (Gedan et al., 2011), mimicking processes in a natural marsh edge (Bilkovic & Mitchell, 2013). Unlike hardened shorelines, it is the vegetation that allows marshes and living shorelines to continuously maintain pace with sea level rise through sediment accretion (Mitchell & Bilkovic, 2019). Living shorelines have been proven to prevent further coastline erosion and in some cases reversed its effects (Swann, 2008; Polk & Eulie, 2018).

The goal of this study was to investigate the effects of three different shoreline types (natural marsh, living shoreline, and hardened shoreline) on hydrologic, geomorphic, and vegetation conditions by synthesizing data collected at six representative living shoreline study sites along the northern Gulf of Mexico. The objectives were to: (1) collect and compare data on hydrologic features, including wave power and turbidity, (2) determine geomorphic features, including slope and sediment composition, (3) determine the abundance and diversity of shoreline vegetation for the three shoreline types, and (4) synthesize these various data into a conceptual model to facilitate identification of shoreline conditions where living shoreline projects are more likely to be successful.

Methods

Study Sites

This study occurred at six different sites along the Mississippi and Alabama coastlines of the Gulf of Mexico, U.S.A. (Figure 1). Sites were sampled in the summer and winter of 2020. Sites that were categorized as high energy sites included: Alonzo Landing (AL) and Swift Tract Project (ST) in Alabama, and the Hancock County Marsh Project (HC) in Mississippi (Figures 1, 2). Sites categorized as low energy sites were Camp Wilkes (CW), Ocean Springs Inner Harbor (OS) and Bayou Heron, Grand Bay NERR (GB) in Mississippi (Figures 1, 2). The oldest of the living shorelines was at AL (constructed in 2005, Swann, 2008), followed by GB (2007, Sparks et al., 2013), HC (2015, NOAA 2013a), ST (2016, NOAA 2013b), OS (2017, NOAA, 2016), and CW (2018, Sicango et al. 2021). With the exception of AL and GB, all living shorelines were created within five years of field sampling. At each of the six sites, we sampled three adjacent shoreline types: (1) natural marsh (NS), (2) living shoreline (LS), and (3) hardened shoreline (HS). At each location, we characterized: (1) hydrologic features, (2) geomorphic features, and (3) vegetation abundance (Figure 3).

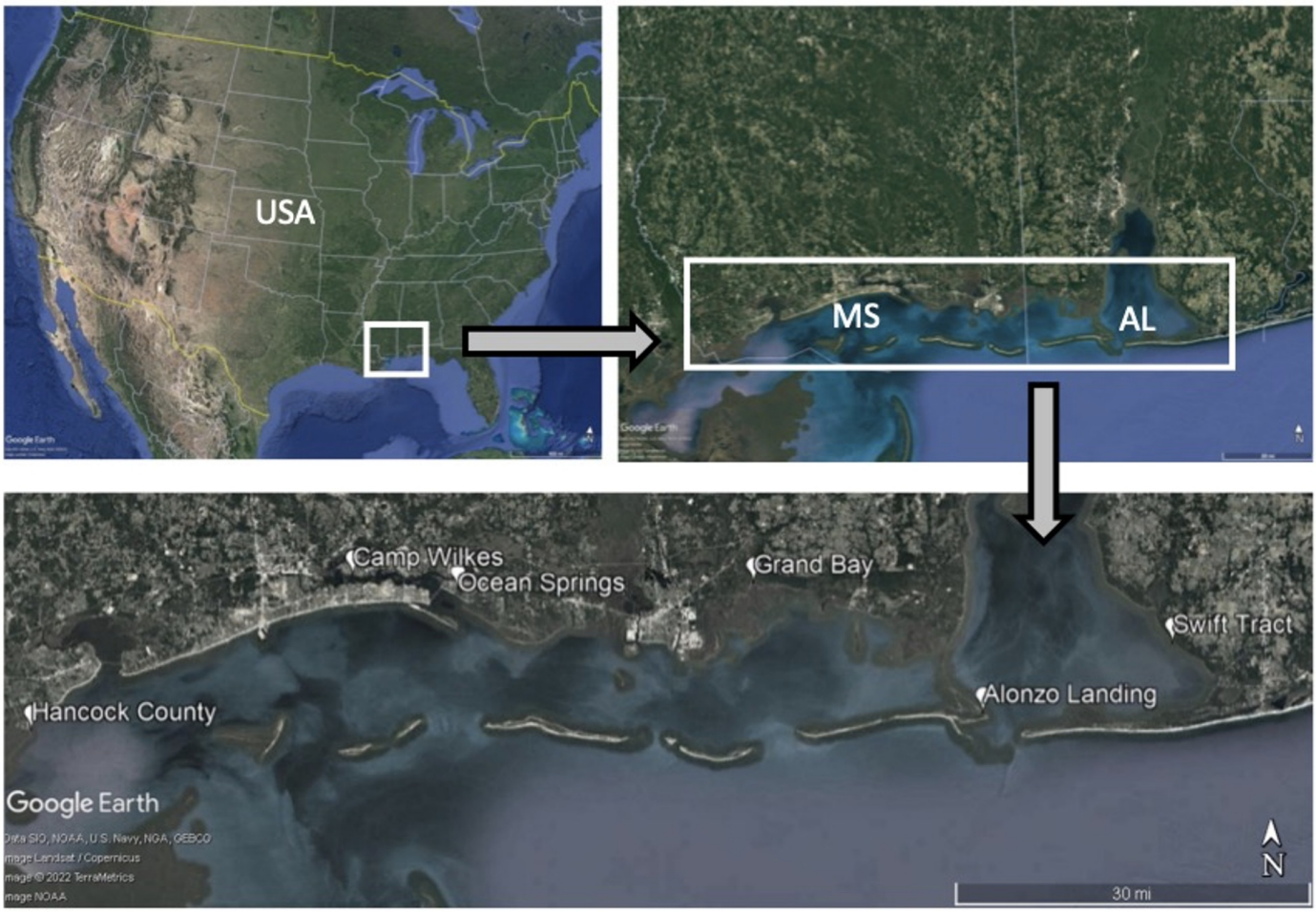

Figure 1. Map of the six study site sites in Mississippi and Alabama, U.S.A. Each site has three shoreline types (natural, living, and hardened shoreline).

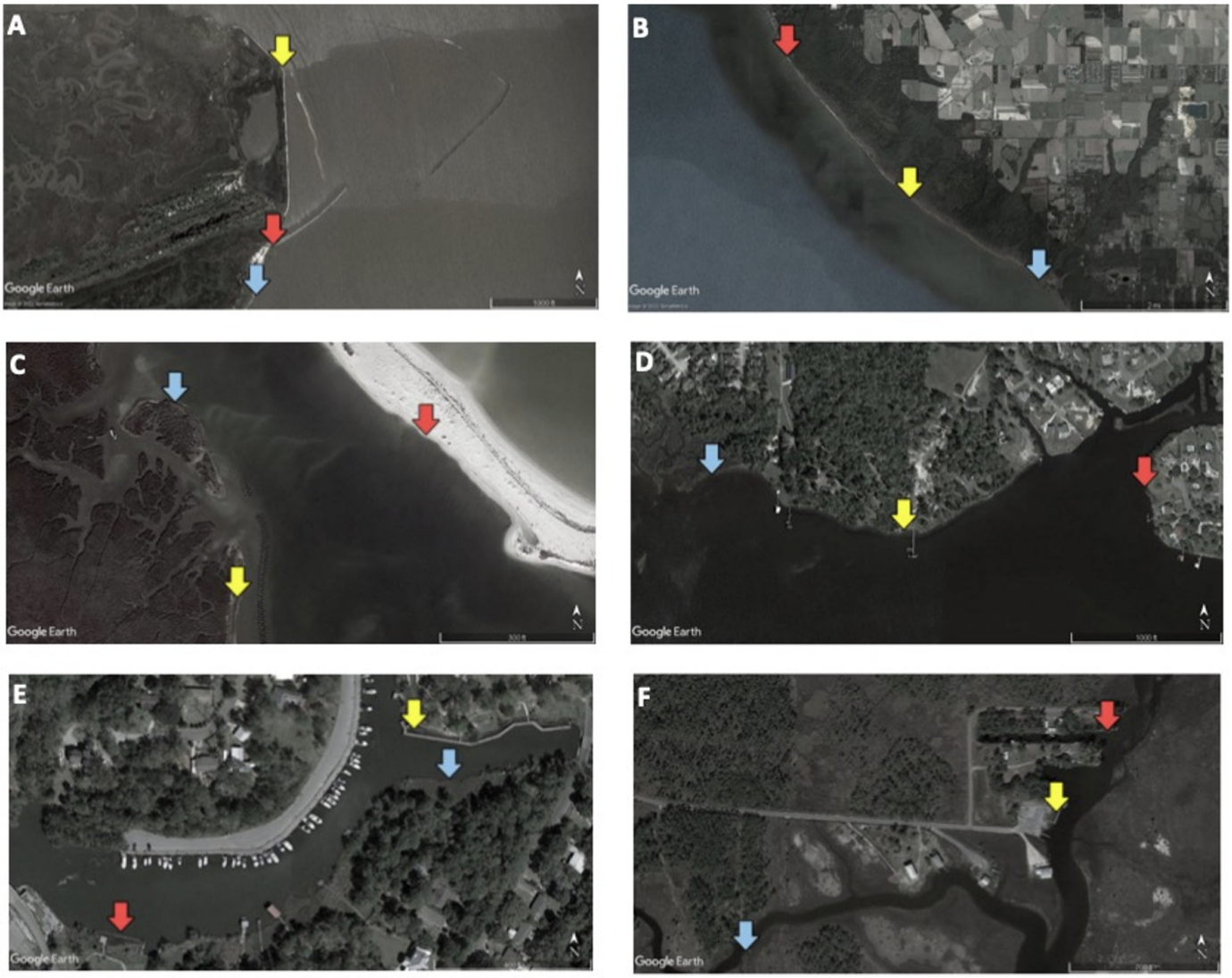

Figure 2. The natural shoreline (blue arrow), living shoreline (yellow arrow), and hardened shoreline (red arrow) at the six study sites. The high energy sites are Hancock County Marsh (A), Swift Tract (B), and Alonzo Landing (C). The low energy sites are Camp Wilkes (D), Ocean Springs Inner Harbor (E), and Grand Bay NERR (F).

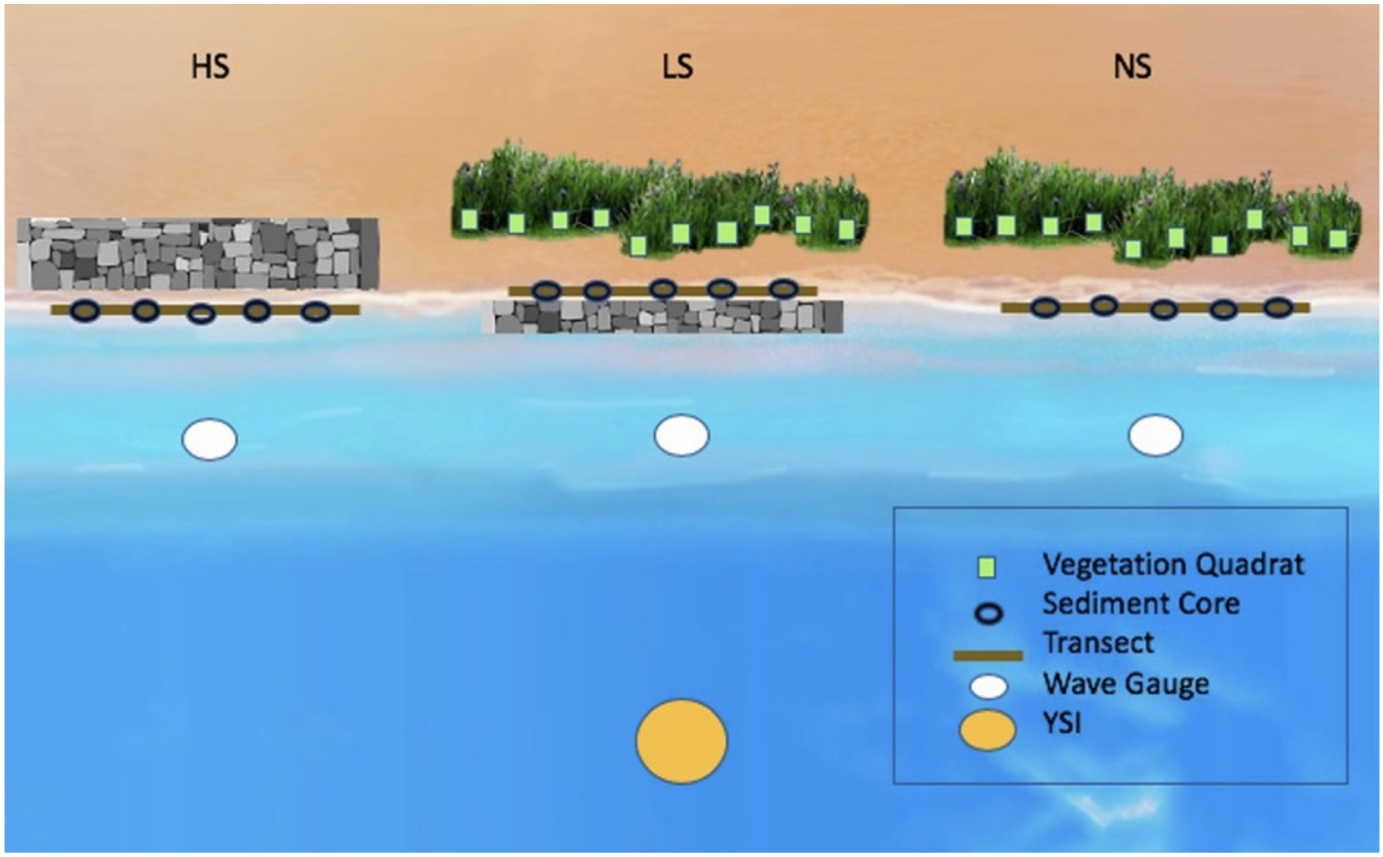

Figure 3. Schematic showing the spatial layout of sampling methods at each of the six sites. Wave gauges (n=3) and YSI (n=1) were deployed in the winter and summer at each site. Sediment cores (n=5) were collected in the winter, and vegetation quadrats (n=10) were collected in the summer along a transect line parallel to the shoreline at each of the HS, LS, and NS shoreline types.

Hydrologic Features

The hydrologic factors we measured include wave pressure using gauges to collect wave power recorded at 1 Hz Frequency (Temple et al. 2021). We also used calibrated YSI 6600 series sondes to collect turbidity, temperature, conductivity (salinity), and dissolved oxygen recorded at 15 min intervals during 5 – 10 day unattended logger deployments (Figure 3). At each of the six sites, a wave gauge was placed in front of each of the three shoreline types with a single YSI between them. Measurements were collected during two seasons (winter 2019 and summer 2020). Loggers were placed between 5 and 30 m offshore from each of the three shoreline types depending on the slope to ensure recording occurred at a similar depth.

Geomorphic Features

The geomorphic factors we measured included relative exposure, shoreline erosion rate, and slope, as well as sediment bulk density, organic content, and grain size distribution derived from in-situ sediment cores. Relative exposure was calculated using fetch distance integrated along 16 bearing lines following the method of La Peyre et al. (2014). Long-term (multi-annual) erosion rates were measured for all three shoreline types at each of the six sites by Juneau (2021) using a simplified Digital Shoreline Analysis System - DSAS approach (Himmelstoss et al., 2021). Shoreline retreat distances

from the DSAS were then used to determine the average rate of erosion per year between 2011-2019. Slope change at the water line was measured from duplicate elevation survey transects recorded at 1 m intervals and used to create elevation profiles up to 10 m inland and 10 m offshore from the water line (Juneau 2021).

Sediment was collected in the subtidal flats immediately adjacent to the shoreline vegetation or hardened structure. At each of the three shoreline types within a site, we collected five sediment cores along a 50-100 m long transect running parallel to and approximately two meters offshore from the marsh vegetation shoreline or bulkhead (Figure 3). To collect the sediment samples, we used a PVC corer with a diameter of 5.08 cm (2”). The coring device was pushed to a soil depth of 30 cm, then removed and the core carefully extruded intact. Each core was separated into three depth strata: shallow (0-10 cm), mid (10-20 cm), and deep (20-30 cm), and each stratum was placed in a labeled and sealed plastic bag on ice, returned to the lab, refrigerated, and processed as soon as possible. To process the sediment sample, the content of each bag was homogenized and then split into two subsamples to measure bulk density (BD), organic matter (OM) content, and grain size.

Subsample #1 – Bulk density and organic matter content: BD was calculated as mass/volume from an initial subsample of 1.5 tbs (22 ml) of the homogenized sediment. The subsample was placed in an oven to dry at 70-80 °C. Once a constant weight was achieved it was then combusted in a muffle furnace at 550 °C for four hours to determine OM content by subtracting the ash-free dry weight (AFDW) from the dry weight.

Subsample #2 – Sediment grain size: The remaining sediment in the bag was weighed and then wet sieved to separate the sand, fine sand, and silt-clay fractions using # 10 (2 mm – large debris), #18 (1 mm - coarse sand) and #230 (0.625 mm – fine sand) stacked sieves, allowing the silt and clay to pass through. Water was run through the stacked sieves to separate the sediment fractions until the water ran clear. The sample wet and dry weights were then recorded for the sediment fraction remaining in each of the sieves. Sample silt/clay content was inferred from the difference in remaining sample weight after sieving, subtracted from the initial total subsample weight before sieving.

Vegetation Surveys

Vascular plant abundance was measured in ten replicate 1 m^2 quadrats spaced equidistant along a 50 m long transect running parallel to shore and located 3 - 5 meters upslope from the vegetated edge during spring/summer 2020 (Figure 3). Since there were no plants downslope along hardened structures, vegetation for these shorelines was recorded on the landward side only when there was vegetation present. The percent cover for the entire quadrat and for each of the dominant plant species was recorded. Unknown plants were collected and brought back to the lab where they were then identified using taxonomic guides for the northern Gulf of Mexico (Correll and Johnston 1970; Radford et al. 1983; Clewell 1985). The average percent cover of marsh vegetation was also calculated based on the nine species that Eleuterius (1972) identified as dominant marsh plant species in Alabama and Mississippi; these include *Juncus roemerianus, Sporobolus alterniflorus (*syn. *Spartina alterniflora), Spartina patens, Spartina cynosuroides, Distichlis spicata, Sagittaria lancifolia, Fimbristylis castanea, Schoenoplectus americanus,* and *Bolboschoenus robustus.*

Data Analysis

Data collected from the wave gauges were analyzed in MATLAB using code from Temple et al. (2021) to calculate the average wave power (kW/m); statistical analysis used the non-parametric Kruskal–Wallis test. Turbidity data from the YSI was analyzed by two-way ANOVA using the factors: site & season and wave power group & season. Sediment data analysis included the calculations for BD, OM content, and sediment grain size composition. For each of these parameters, a two-way ANOVA was performed using the factors: site & shoreline and wave power group & shoreline. Vegetation analysis included two-way ANOVA for species richness, average percent cover, and diversity calculated using the Shannon-Wiener H and Simpson D indices using the R package Vegan (Oksanen et al. 2020). Factors with a significant response (alpha $\leq$ 0.05) were followed by a Tukey's honestly significant difference (HSD) post-hoc test to find groupings with statistically similar means. Finally, multivariate non-parametric multi-dimensional scaling ordination (nMDS) and principal components analysis (PCA) were used for further data exploration and synthesis. The data for both ordinations were centered to mean zero and standardized to unit variance. All data analysis was done in R using RStudio (ver. 1.9, Boston, MA).

Results

Hydrologic Features

Wave gauge data were used to determine the energy exposure for the six sites. Average wave power was significantly different among the six sites ($H_5 = 21.49, p < 0.00$) with post-hoc tests indicating two significantly different ($H_1 = 19.36, p < 0.00$) groups. The resulting high and low energy groupings were: (1) the high energy sites: HC, ST, and AL, and the low energy sites: CW, OS, and GB (Table 1). The average wave power for the high energy sites was over five times greater than that at the low energy sites (Table 1). The various parameters recorded by the wave gauges all had similar trends to the average wave power (see Appendix B), which reflected the amount of wave forces that impacted the shorelines and contributed to the erosion of sediments.

Turbidity was significantly different between winter and summer among the six sites ($F_{1, 5} = 88.40, p < 0.00$). AL and HC varied the greatest between the two seasons, with AL having a higher turbidity in the winter and HC having a higher turbidity in the summer. When comparing across sites using both seasons, HC had the highest turbidity of all sites and the lowest was at OS. The mean turbidity of the high energy sites was over five times greater than the mean turbidity of the low energy sites (Table 1). These results for the turbidity data indicate that it is influenced by both energy grouping and site-specific variables. Turbidity may also be influenced by relative exposure and wave power, as well as sediment grain size at the site, with finer-grained sediments resulting in more frequent and intense turbidity.

Table 1. Average wave power (kW/m) and YSI water quality data include mean (± SE) for turbidity (NTU), temperature (^{o}C), salinity (ppt), and dissolved oxygen (D.O.) concentration (mg/L) for two seasons. Significant differences in means are indicated by superscript letter groups.

Site	Avg Wave Power	Season	Turbidity	Temperature	Salinity	D.O. conc
High Energy	6.9 ± 0.95[a]	Winter	18.6 ± 0.89	13.2 ± 0.06	8.8 ± 0.05	8.4 ± 0.09
		Summer	17.7 ± 0.95	28.7 ± 0.04	9.9 ± 0.04	1.8 ± 0.08
Low Energy	1.3 ± 0.23[b]	Winter	3.1 ± 0.08	14.5 ± 0.04	14.6 ± 0.10	6.6 ± 0.07
		Summer	3.7 ± 0.07	29.6 ± 0.07	8.4 ± 0.11	3.0 ± 0.13

Geomorphic Features

The relative exposure at each of the six sites was influenced by their orientation to the dominant seasonal wind direction, which comes primarily from the SE direction. Sites exposed to the dominant seasonal winds across a long fetch experienced the highest relative exposure, notably, these included HC and ST (Table 2). The mean relative exposure was significantly different among the six sites ($F_{5,\ 1130} = 59.57, p < 0.00$). The relative exposure at HC was significantly greater than at all other sites (Table 2). The mean relative exposure was significantly different between the two energy groups ($F_{1,\ 1134} = 98.94, p < 0.00$). The high relative exposure sites were also the high wave energy sites and included HC, ST, and AL; all had significantly greater relative exposure than the low wave energy sites that included CW, OS, and GB (Appendix B). This finding suggests that relative exposure at a shoreline may be strongly influenced by the cardinal direction of seasonally dominant winds interacting with fetch distance and shoreline orientation. The highest relative exposure occurs when a shoreline is facing perpendicular to a long fetch distance that is also in the direction of the strongest seasonal winds. This allows the formation of large waves that crash onto the shoreline and can cause rapid edge erosion.

Table 2. Average (± SE) relative exposure for natural, living, and hardened shoreline types in each wave power energy group and for all shoreline types. Significant differences in means are indicated by superscript letter groups.

Energy	Natural	Living	Hardened	All Types
High	3,869 ± 1,092	4,070 ± 1,127	3,857 ± 1,184	3,932 ± 636.6[b]
Low	121 ± 41.3	118 ± 41.7	106 ± 42.1	115 ± 23.4[a]

Sediment Bulk Density and Organic Matter Content

Bulk density (BD) and organic matter (OM) at each shoreline type within the site were calculated by averaging the sediment core data obtained over the three depth strata. The mean BD was significantly different ($F_{2,262} = 66.53, p < 0.00$) among the three shoreline types: natural shoreline (NS), living shoreline (LS), and hardened shoreline (HS). Bulk

density was lowest in the NS and highest in the HS. This indicates that the NS had the most permeable sediments followed by the LS, while the HS had the least permeable and most compacted sediments, which can stunt vegetation root growth. Shoreline type can significantly influence the BD of intertidal sediments. The mean BD was not significantly different ($F_{1, 259} = 1.006, p < 0.32$) between the two energy groups (Table 3). The highest overall BD was found at the HS in high energy sites. Even in the higher energy sites, the BD at the NS and LS was similar to the NS at the low energy sites, with more permeable sediment allowing the roots to grow better, and it may be expected for these shorelines to have finer organic-rich sediment particles. This finding indicates that BD may be influenced both by the type of shoreline and the amount of energy that a shoreline receives.

Table 3. Average (± SE) of the sediment BD and OM collected from sediment cores at three shoreline types within the high and low energy groups respectively. Significant differences in means are indicated by superscript letter groups.

Shoreline	Bulk Density (g/cm^3)	Organic Matter (%)
High Energy		
Natural	0.62 ± 0.05^{a}	17.3 ± 1.45^{b}
Living	0.70 ± 0.06^{a}	23.7 ± 3.89^{b}
Hardened	1.34 ± 0.03^{c}	1.47 ± 0.38^{a}
Low Energy		
Natural	0.58 ± 0.07^{a}	18.5 ± 2.24^{b}
Living	1.08 ± 0.06^{b}	5.58 ± 0.81^{a}
Hardened	1.16 ± 0.06^{bc}	4.28 ± 0.46^{a}

The mean OM was significantly different among the three shoreline types: NS, LS, and HS ($F_{2, 262} = 28.68, p < 0.00$). The OM at HS was significantly lower than the other two shoreline types (Table 3), which indicates there is little organic content in HS sediment. The LS had over five times as much organic matter and NS had over six times as much organic matter as the HS. This indicates that the OM content of the sediment may be positively influenced by having marsh vegetation present (NS and LS).

The mean OM was significantly different between the two energy groups ($F_{1, 259} = 7.685, p < 0.006$). The OM in the high energy NS and LS sites was higher than the OM at HS sites. The OM in the low energy LS was less than in the high energy LS sites (Table 3), however, OM at LS shorelines in both energy groups was still greater than the HS shoreline type. This finding indicates that the energy groups may not influence OM in NS or HS, but they do at the LS.

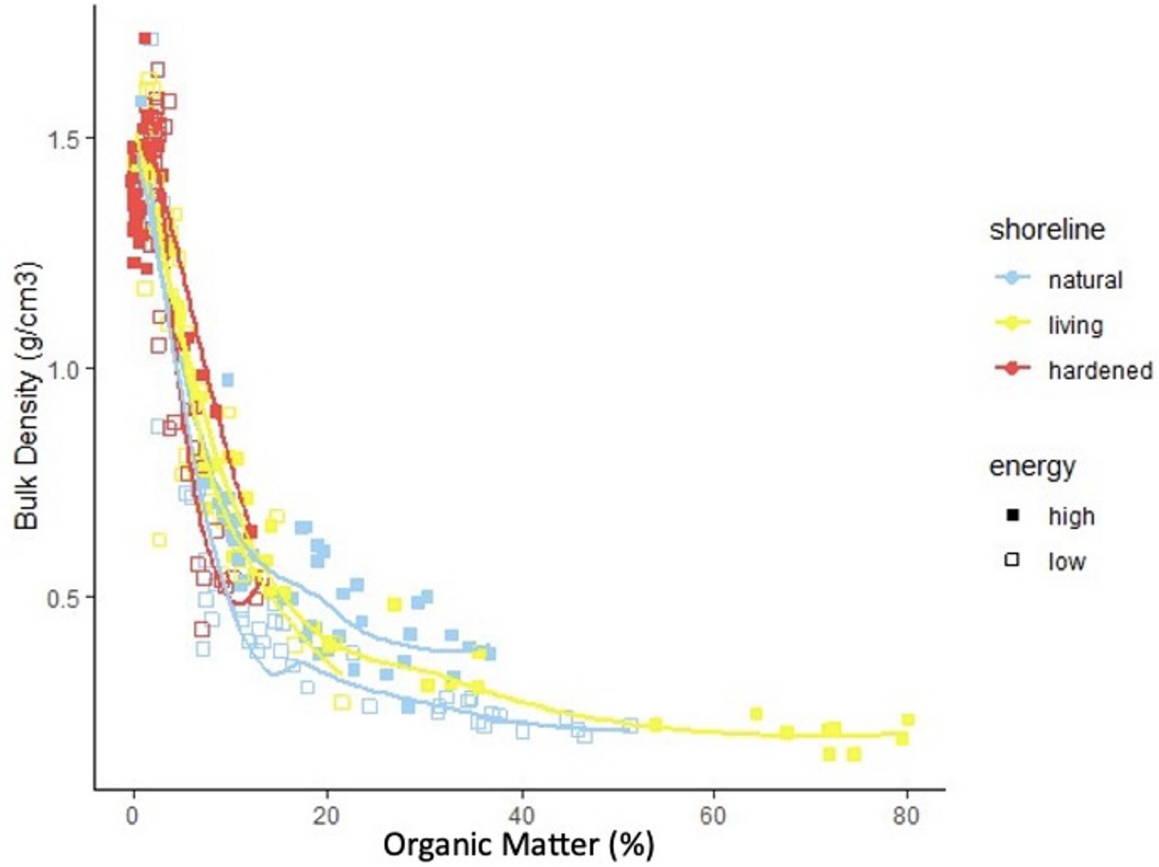

Figure 4. Interaction of OM with BD for all samples from the two energy groups and three shoreline types. Symbols and colors indicate sample origin, filled symbols indicate high energy sites and open symbols indicate low energy.

The scatterplot (Figure 4) shows that BD and OM have an inverse relationship with OM declining as BD increases. The HS (red points) clustered together and had higher BD and lower OM, the LS (yellow points) had the greatest variability, and the NS (blue points) generally had lower BD and higher OM than the HS. The BD, averaged by shoreline type, exhibited an increase from NS and LS to HS. The low energy sites had higher OM at the NS compared to LS and HS. In contrast, the high energy sites had lower OM at the HS, compared to the other two types. The high energy LS sites had an 18 % increase in OM compared to the respective low energy LS sites.

Sediment Grain Size

Sediment grain size composition changed with depth in the top 30 cm, with the percent sand declining and silt/clay increasing with depth; percent coarse sand remained low (<10%) and was not influenced by depth. These results suggest sand grains were more abundant in the upper portion of the sediment cores, potentially because of wave energy winnowing the finer silt and clay particles, which tend to accumulate at deeper depths (>10cm) or are transported to lower energy conditions in deeper water depths offshore. The three sampling depths were combined for the remaining sediment grain size analysis.

When sediment grain size data was analyzed by shoreline type (NS, LS, and HS), the NS had the highest percentage of

silt/clay (Table 4, Figure 5). The silt/clay fraction was lowest at the HS sites and the sand content was highest (Table 4). Sand was the dominant sediment grain size in both HS and at some LS, and lowest at the NS shoreline type. Sediment composition at the six sites differed significantly for the percent of coarse sand and pebbles ($F_{5, 258} = 2.92$, $p = 0.01$), sand ($F_{5, 258} = 9.52$, $p < 0.00$), and silt and clay ($F_{5, 258} = 9.43$, $p < 0.00$) size fractions, primarily based on the high and low energy groupings. The sand fraction in both energy groups decreased from the HS to NS, and the sand fraction was greater in the HS high energy sites than at the low energy sites (Table 4). The silt/clay fraction increased from HS to NS, with LS intermediate. The NS had less than a one percent difference of silt/clay between the high and low energy sites (Table 4), while the HS had a ~30% difference with high energy sites containing less silt/clay than the low energy sites. Percent sand exhibited an inverse relationship to the percent silt and clay across both energy groups. The HS in the low energy sites was an exception, having a slightly higher percent silt and clay than the corresponding LS.

Table 4. Average (± SE) of three sediment size fractions collected from sediment cores at three shoreline types within the high and low energy groups respectively. Significant differences in means are indicated by superscript letter groups.

Shoreline	Coarse Sand (%)	Fine Sand (%)	Silt and Clay (%)
High Energy			
Natural	2.96 ± 0.55^{b}	37.1 ± 4.49^{a}	59.9 ± 4.75^{c}
Living	5.37 ± 0.77^{ab}	60.8 ± 4.15^{b}	34.2 ± 3.89^{b}
Hardened	3.92 ± 0.95^{ab}	92.7 ± 1.84^{c}	3.83 ± 1.06^{a}
Low Energy			
Natural	8.67 ± 2.31^{a}	33.3 ± 3.22^{a}	59.4 ± 3.50^{c}
Living	4.04 ± 0.55^{ab}	70.6 ± 3.26^{b}	25.3 ± 3.13^{b}
Hardened	4.74 ± 1.01^{ab}	60.6 ± 3.12^{b}	34.6 ± 3.07^{b}

Sediment grain size data indicated that the sand vs. slit/clay fractions were the major change observed in the sediment composition across all sites and shoreline types. There was an inverse relationship between these two grain size classes, with higher sand content resulting in less silt/clay and vice versa. The sand fraction was higher in the shallow (<10cm) portion of the sediment core across all six sites. The sand fraction was greater at the HS and reduced at the LS and NS, with the NS shoreline type generally having the largest silt/clay fraction. Finally, high energy sites tended to have more sandy sediments than low energy sites, presumably as a result of the increased wave action.

Figure 5. Sediment grain size composition at three shoreline types within the high and low energy groups respectively. Significant differences in means are indicated by superscript letter groups for the different sediment size fractions (pebbles, sand, and silt).

Vegetation Diversity and Cover

A total of 39 plant species were found within the 180 quadrats sampled (Appendix A - Table A1). The native vegetation of the Mississippi-Alabama Gulf Coast saltmarshes is dominated by *Juncus roemerianus* Scheele and *Sporobolus alterniflorus* (Loisel) P.M. Peterson & Saarela (syn. *Spartina alterniflora*). Other common marsh species include *Spartina patens* (Aiton) Muhl, *Spartina cynosuroides* (L.) Roth, *Schoenoplectus americanus* (Pers.) Volkart ex Schinz & R. Keller, and *Distichlis spicata* (L.) Greene (Bilkovic & Mitchell, 2018; Eleuterius 1972). Species richness was not significantly different among the six sites ($F_{5,174} = 1.75$, $p = 0.20$) or among the three shoreline types ($F_{2,175} = 0.18$, $p = 0.86$), this could be because the HS had both the highest (CW) and lowest (HC and AL) number of species. All 17 species found at the CW HS were upland trees and shrubs, that were not found at either the CW NS or LS marsh sites, accounting for the high species variability at CW. In comparison, the HS at HC and AL sites had no species recorded as sampling occurred on rock seawalls that precluded vegetation growth. Species richness was significantly different between the two energy groups ($F_{1,178} = 5.43$, $p = 0.03$), with species richness for the low energy sites ~50 % higher than at the high energy sites. The site with the highest species richness was CW (28 species), and the lowest was ST (5 species) (Table 5). These results indicate that species richness may be influenced by the energy groups, with low energy conditions tending to increase the number of plant species found. Simpson's D and the Shannon Weiner H diversity indexes placed the energy/shoreline combinations in a similar order as the species richness data (Table 5). Across groups, there was higher variability in diversity at HS and less variability at NS and LS for both the Simpson's D and the Shannon Weiner H indexes (Table 5). The high energy HS sites had 0-1 species and the low energy HS sites had 7-17 species with varying composition, depending on the type of hardened shoreline installed and whether forested upland vegetation occurred upslope.

Table 5. Vegetation data by energy groups and shoreline type for species richness, and the average (± SE) total percent cover, dominant marsh species cover, the Shannon Wiener H index, and Simpson's D diversity indexes. Significant differences in means are indicated by superscript letter groups.

Shoreline	Species Richness	Total Sp. Cover (%)	Marsh Sp. Cover (%)	Shannon H Index	Simpson D Index
High Energy					
Natural	10	61.7 ± 4.78^{b}	58.3 ± 5.97^{b}	1.20	0.59
Living	10	63.3 ± 5.17^{b}	57.2 ± 9.31^{b}	1.65	0.73
Hardened	1	31.7 ± 8.32^{a}	0.00 ± 0.00^{d}	0.00	0.00
Low Energy					
Natural	10	72.8 ± 3.11^{b}	71.5 ± 4.76^{a}	1.52	0.72
Living	18	66.7 ± 4.08^{b}	49.4 ± 7.40^{bc}	1.74	0.75
Hardened	25	60.2 ± 5.19^{b}	35.1 ± 22.8^{c}	2.35	0.87

Vegetation percent cover was significantly different among the three shoreline types ($F_{2, 177} = 8.84$, $p < 0.00$). The NS had the highest average percent cover, but the HS was significantly lower. The NS and LS tended to have higher average percent cover because both are characterized by dominant marsh vegetation or were planted soon after construction. The

HS at both HC and AL contained no vegetation as the sampling transect was on a rock sea wall. These findings indicate that the percent cover of vegetation may be affected by humans building a hardened structure. Vegetation percent cover was significantly different between the two energy groups ($F_{1, 178} = 9.93$, $p < 0.00$). The low energy sites had a higher percent cover of vegetation than the high energy sites (Table 5). These results show that both shoreline type and energy may affect the percent cover of vegetation. Vegetation percent cover was also significantly different among the six sites ($F_{5, 174} = 8.79$, $p < 0.00$), with the highest average percent cover found at OS and the lowest percent cover at HC.

Nine of the species recorded are considered dominant marsh species in Mississippi by Eleuterius (1972). There was a significant difference between the shoreline types in the percent dominant marsh species present ($F_{2, 177} = 46.03$, $p < 0.00$). The NS had the highest percentage of dominant marsh species but was significantly different from the HS with the fewest. The percent of dominant marsh species was significant among the different energy groups ($F_{1, 178} = 17.14$, $p < 0.00$). The highest percent of dominant marsh species was at the low energy NS, while the lowest was at the high energy HS (Table 5). This finding shows that energy and shoreline type play a role in the percentage of dominant marsh vegetation found.

Data Interactions

To visualize data interactions among the different factors (hydrologic, geomorphic, and vegetation) an nMDS (Figure 5) and a PCA ordination were conducted (Figure 6). Hydrologic features that were included in both the nMDS and the PCA were the average wave power and turbidity. The geomorphic features included were relative exposure, average erosion rate, average slope, percent sand, and organic matter. The vegetative features included were species richness, percent cover of dominant species, and total percent cover.

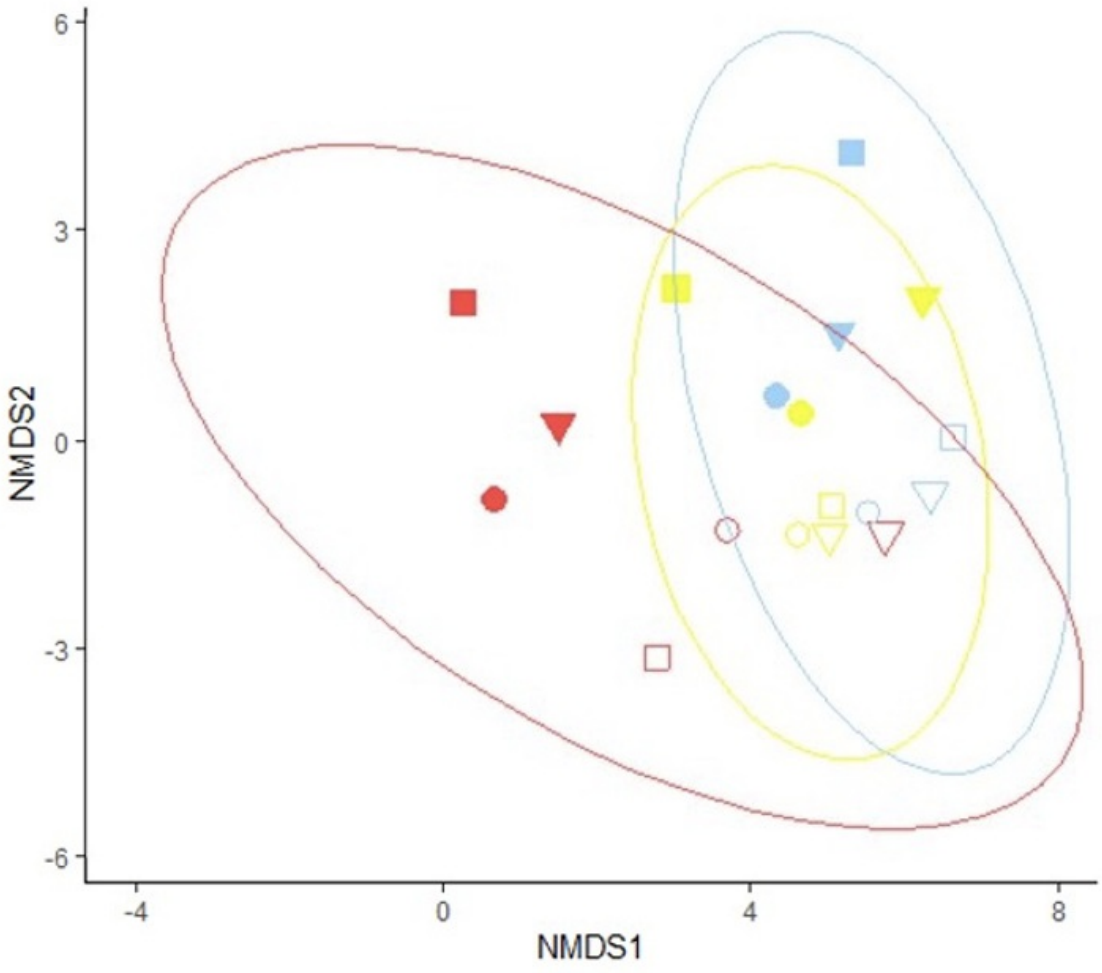

Figure 5. Non-metric multidimensional scaling plot (k = 2, stress= 0.95) for the three shoreline types (NS = blue, LS = yellow, HS = red) and two energy groups. High energy sites have solid shapes, while low energy sites have open symbols with their corresponding 95% density ellipses.

The nMDS and the PCA show similar patterns in the dataset (Figures 5 and 6). In the nMDS, there is a substantial overlap between the NS and the LS sites. The low energy HS sites overlap with the NS and LS density ellipses in the bottom right quadrant. However, the three high energy HS sites vary greatly from either the NS or LS. The nMDS1 axis shows a separation by the type of shoreline, while the nMDS2 axis shows separation along the different energy groups (Figure 5).

In the PCA, approximately 76% of the estimated variance is explained by the first three principal component axes, the first axis (PC1) explains 35.9%, the second axis (PC2) explains 31.0%, and the third axis (PC3) explains 8.7% of the estimated variance in the dataset. The PC1 axis represents the percent of dominant vegetative species, the percent cover of vegetation, and the average slope of the shoreline. This axis shows a pattern of high energy groups at the HS to low energy groups at the LS and NS. PC2 represents turbidity, erosion rate, relative exposure, and average wave power. This axis mostly represents energy and the geomorphic shape of the shoreline, it shows a gradient between low and high energy groups as well as from HS to NS. PC3 represents primarily species richness. This axis shows the vegetation diversity at the low energy HS is similar to the NS and LS in the high energy sites. The PCA plots indicate the LS and NS

are substantially similar to each other and they both have a strong separation from the high energy HS sites (Figure 6). Generally, there is a separation of the high energy sites across the three shoreline types, while the low energy sites are more grouped together.

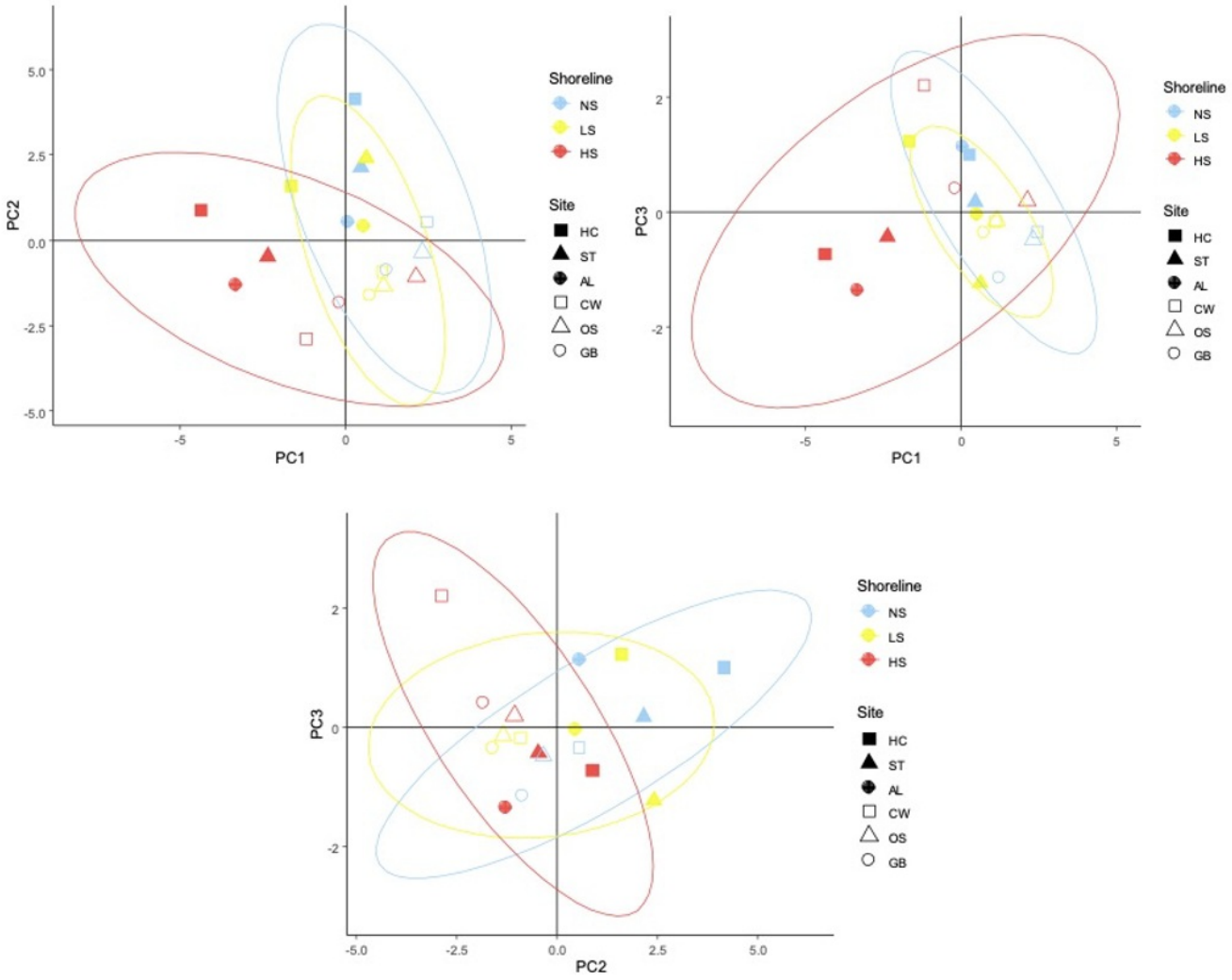

Figure 6. Principal Component Analysis for the three shoreline types at each site. High energy sites have solid shapes, while low energy sites have open symbols with their corresponding 95% density ellipses.

Discussion

This study looked at natural, living, and hardened shorelines occurring in two different energy groups to determine how the hydrologic, geomorphic, and vegetative processes may respond to environmental conditions. Predominantly the high vs. low wave energy conditions at a shoreline influenced all the other variables studied. Shoreline type (NS, LS, HS) influenced the erosion rate, slope, sediment variables, and the total percent cover, and percent of dominant marsh species present. Site-specific conditions also played a role in many of the variables measured.

Hydrologic Features

The hydrologic data used average wave power to group the six sites into high (HC, ST, and AL) and low energy (CW, OS, and GB) sites. At the high energy sites, the average wave power was five times greater than at the low energy sites, and this division was used in further analysis. Wave energy and erosion have a linear relationship (Leonardi et al., 2016) and this may help to indicate the wave energy conditions under which the different types of shorelines occur. Studies have shown that shorelines that receive lower wave energy are less likely to require human intervention, although conditions at some sites may be exacerbated by human development activities (Erdle et al., 2006). We used the average wave power because it shows the amount of wave forces a shoreline is receiving, but adoption of this method would depend on access to relevant equipment and field sampling capabilities. A suitable alternative to using the average wave power could be turbidity when water quality sampling is already available.

Measuring turbidity indicates the number and type of particles in the water column, usually positively influenced by rougher water conditions. High wave energy can disturb the sediment, suspending it into the water column, however, vegetation can reduce this disturbance since the root biomass stabilizes the sediment (Bilkovic et al., 2016), and emergent stems can reduce water velocities (Gedan et al., 2011). The high energy sites were found to have almost five times greater turbidity than the low energy sites. The turbidity and wave power were highly correlated (r^2 = 0.85), showing a strong positive relationship between them.

Geomorphic Features

The relative exposure was calculated using the method of La Peyre et al. (2014) to explain the wave power and turbidity found at each site based on fetch distance, wind speed, and wind direction. According to Erdle et al. (2006), sites with a maximum fetch distance of less than 800 m (~0.5 mi) are considered low energy and less likely to require living shoreline protection, although other factors could exacerbate local erosion (Duhring et al., 2006). Half of the sites in our study fit that criterion, with three low energy sites: AL (298 m), GB (108 m), and OS (107 m); while the other three sites would be considered high energy: HC (31,944 m), ST (56,663 m) and CW (1,485 m). This contradicts the wave energy groups we found because AL and CW are switched, implying that there may be other local factors affecting the wave energy exerted on these two specific shorelines.

Shorelines with high relative exposure also experienced more rapid shoreline erosion rates from 2011 to 2019. The highest mean annual erosion rate over this eight-year period averaged over all six sites, was the NS type (Juneau 2021; Spellmann 2022). The NS (0.70 m/yr) had a higher erosion rate than either the LS (0.25 m/yr) or HS (-0.02 m/yr). It was expected apriori that the HS would have little to no erosion because it is engineered to be a permanent structure. The high erosion rates at the NS were also expected as most of the NS had a scarp at the vegetation base indicative of existing prior edge erosion. The higher scarps found at the high energy NS sites exposed the roots, which previously had helped to contain the sediment before edge erosion became the predominant process (Bilkovic & Mitchell, 2018). The erosion results in this study fit the expectation that LS are a compromise to maintain the natural ecosystem while also reducing the rate of erosion, whereas the HS are a proven technique to completely stop the rate of erosion Polk & Eulie, 2018).

Shorelines with steeper slopes, indicated by larger scarps, reflected the impacts of the higher wave energy and tended to have larger grain-size sediments and higher edge erosion rates (Nelson, 2008). Steep slopes make it more difficult for vegetation to grow and the implementation of a breakwater structure with a living shoreline project helps facilitate conditions suitable for sedimentation and vegetation expansion (Erdle et al., 2006). The mean slopes at the three shoreline types were different, with the HS having a significantly steeper slope than either the NS or LS, which did not differ from each other (Juneau 2021; Spellmann 2022). These findings indicate that shoreline slope is often affected by manmade structures especially in the HS and in some LS sites. Erdle et al. (2006) found that sites with greater fetch may need to have fill added to the shoreline to reduce the steep slope before vegetation can establish. Shoreline slope and mean erosion rates may in turn affect sediment composition, water turbidity, and vegetation found at the site.

Sediment Composition

Sediment grain size and composition influence, and are influenced by, sedimentation rates, bulk density, organic matter, plant growth potential, and benthic organisms (Bilkovic & Mitchell, 2018). Sediment BD is an important indicator of the potential ability of plant roots to grow and expand into the sediments and in coastal areas tends to reflect the percent of sand in the sediment (Vymazal, 2013). The OM content in the sediment reflects the silt/clay content, because the smaller pore space of the finer sediments allows for detrital accumulation and burial (Davis et al., 2015). The NS were found to have the lowest sediment BD, followed by LS and then HS. The inverse pattern was seen for the OM content in the sediments. We found that both BD and OM are not influenced by the energy groups at the NS and HS but were influenced at the LS. For both these parameters, the sediments at the high energy LS sites were more like those of adjacent NS, while at the low energy LS sites, they were more like the sediments of the corresponding HS.

Sediment grain size is affected by the energy that impacts the shoreline, which in turn can affect the ability of vegetation to thrive (Bozek & Burdick, 2005). We found there was a difference in sediment grain size composition based on energy, site, and shoreline type. At the high energy sites, the portion of silt/clay decreased from NS to LS to HS. The results for the high energy shorelines corroborate findings by Mitchell & Bilkovic (2019) that the sediment found at LS will be more similar to those at NS. In contrast, the portion of silt/clay at the low energy sites decreased from NS to HS to LS. The sediment grain size for the low energy shorelines reflects the findings of Feagin et al. (2009), that the higher percentage of sand found at the HS could be caused by scouring at the base of the hardened structures (Basco, 2006; Roberts, 2010). This difference could also be due to the use of sand as fill during construction. The NS had the smallest difference in sediment composition between the high and low energy sites, whereas the greatest difference was found at the HS sites. This finding agrees with Bozek and Burdick (2005) that high energy sites will have coarser, more sandy sediment, as well as Feagin et al. (2009) who found coarser sediment at restored sites.

Vegetation

Vegetation can protect a shoreline from erosion, filter watershed runoff, and provide both food and habitat for different organisms (Craft et al., 2009; Wu et al., 2012; Bilkovic and Mitchell, 2018). The dominant vegetation community is

determined by multiple factors including salinity and wave energy (Bozek & Burdick, 2005; Pennings et al., 2005; Gedan et al., 2011). In the northern Gulf of Mexico saltmarshes, *J roemerianus* is controlled more by physical stress such as salinity and flooding, while *S. alterniflorus* is controlled more through competition (Pennings et al., 2005). The latter is the species most affected by edge erosion, because it is found closest to the water and receives most of the impacts of the wave energy (Eleuterius, 1972). Species richness was found to be affected by energy conditions, with the low energy sites having higher richness. Percent cover was assessed in two ways, total percent cover and the percent cover of the dominant marsh species (Eleuterius, 1972). Total vegetation cover was found to be higher at the low energy sites. The NS and LS were also found to have a higher total vegetation cover than the HS. The dominant marsh species coverage found that both NS and LS had over 55 % cover of dominant marsh species, while HS had less than 15 %. The lower total percent cover and cover by marsh dominant species at the HS removes a vital part of the ecosystem created by a saltmarsh and may endanger species that are endemic to these coastal marshes (Pennings et al., 2005; Bilkovic & Roggero, 2008). Plant diversity varied between the energy groups at the HS, the low energy sites showed higher diversity than the high energy HS sites. In contrast, both the LS and NS had similar diversity trends across both energy groups. There was higher species similarity between the NS and LS especially for the marsh dominant species, but at the HS there was diversity between the high and low energy sites with greater variability in species. The high variability observed in plant diversity at the HS was mostly due to either (1) the removal of all vegetation at rock seawalls or (2) very different upland vegetation behind wooden bulkheads, with either low diversity habitat represented by dense plantings of monospecific turf grasses, or high diversity wooded upland habitat with many plant species present including trees.

Data Interactions and a Conceptual Model

We created a conceptual model (Figure 7) using the PCA ordination results from the six study sites. The ordination results indicate that sites with high turbidity, erosion rates, wave power, and relative exposure had steeper slopes and a higher percentage of sand, but lower total percent cover and percent of dominant marsh species. This conceptual model divides shoreline characteristics into four quadrants. The upper left quadrant (Figure 7A) represents high energy hitting a hardened shoreline with sandy sediment at the base and has no marsh vegetation present. Quadrant B represents a site in high energy with less sand but features a shallower slope with marsh vegetation. Quadrant C is a low energy shoreline but with a steep slope, moderate sand content, and less marsh vegetation. The lower right quadrant (Figure 7D) represents a low energy shoreline, with mostly silt/clay sediments but little sand, and lots of marsh vegetation typical of a natural shoreline. In the conceptual model, the wave energy exerted on the shoreline affects the erosion rate of the coastline resulting in different sediment, slope, and vegetation characteristics found at the shoreline. Shorelines that received high wave energy (Figure 7 A, B) had fewer dominant marsh species and this is probably because they tended to have steeper slopes, often because of armoring, meaning the vegetation present may not be salt or inundation tolerant.

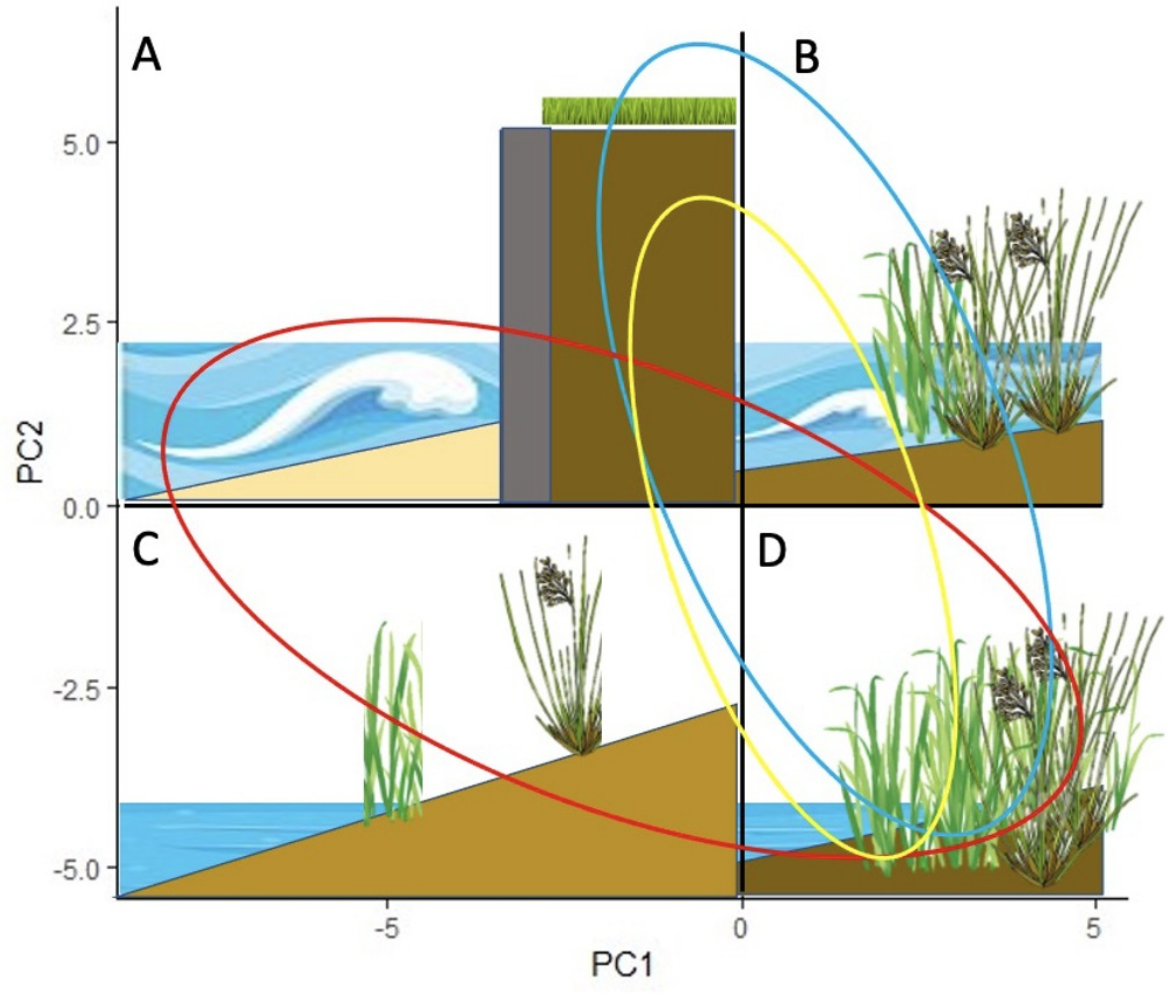

Figure 7. A conceptual model representing the results found in the study sites. The ellipses are from the PCA and show the different types of shorelines: natural (blue), living (yellow), and hardened (red).

In contrast, low energy sites (Figure 7 C, D) had more similar patterns in the response of vegetation, sediments, and slope across the three different shoreline types and were generally more similar to natural marsh shorelines. The NS and LS were characterized by environmental conditions reflected in the lower quadrants (Figure 7 C, D) with shallow slopes that supported higher vegetation diversity and coverage, and sediments with higher organic matter and finer grain sizes. The presence of vegetation and the high sediment organic matter is an important aspect of what makes a natural marsh a key habitat for many species. The LS restorations in the six study sites do appear to provide similar habitat conditions to adjacent reference NS shorelines, and this has also been found in other studies (Bilkovic & Roggero, 2008; Balouskus & Targett, 2016; Partyka et al., 2017).

This conceptual model could be used to help predict sites where the implementation of a LS project will help to retain the shoreline and ecosystem similar to natural marsh conditions within the northern Gulf of Mexico. According to the conceptual model, a living shoreline will do best at a site that is receiving moderate to low energy impacts and has a gradual slope. The gradual slope does not have to be natural; many LS restorations involve the creation of a more gradual slope through sediment infill in conjunction with an offshore breakwater to help stabilize those newly placed sediments

while vegetation establishes.

Conclusions

The goal of this study was to evaluate how hydrologic, geomorphic, and vegetative parameters can affect different shoreline types (natural marsh, living shorelines, and hardened shorelines). This study evaluated six established living shoreline restorations across a range of coastal exposures to identify conditions where a living shoreline project may be most effective. Site selection for living shorelines is a crucial factor that relies on multiple elements (Arkema et al., 2013; Bayraktarov et al., 2015). We conclude that the amount of energy impacting a shoreline is a good proxy for the environmental conditions where implementation of a living shoreline can provide a potentially beneficial outcome. In general, low energy coastlines exhibited less turbidity, less erosion, sediments with a higher percent of silt/clay, more sediment organic matter, and a higher diversity and percent cover of vegetation. High energy sites exhibited a greater variability in the responses of these factors than did the low energy sites.

Wave energy is not the only major component influencing living shoreline stabilization, for instance slope angle, sediment supply and space for vegetation to retreat upslope have also been reported as important (Doody, 2004; Herbert et al., 2018; Mitchell & Bilkovic, 2019). The main difference we found between NS and LS in this study was that the LS had a lower erosion rate. The LS restorations did not stop erosion completely but did lessen the erosion rate compared to the adjacent NS controls. Other than erosion rates, the LS and NS were similar in slope, sediment grain size, soil BD, OM content, percent cover of vegetation, and the percent of dominant marsh vegetation. This study showed that a LS is a potentially good alternative to help maintain a similar ecosystem to the NS while also slowing erosion rates. This research has increased our knowledge of what environmental conditions may be most suitable for living shorelines to help to decrease coastal erosion rates along the northern Gulf of Mexico. Further studies could help weigh the benefits to habitat and property of maintaining the different types of shorelines and their effectiveness at protecting against erosion losses.

Appendix A

Table A.1. List of all 39 plant species found at the six different sites.

Abbreviation	Species Name	Common Name
AMAR	*Amaranthus spp.*	NA
ASTE	*Aster spp.*	NA
BAHA	*Baccharis halimifolia*	Groundsel tree
BAMO	*Bacopa monnieri*	Water hyssop
BOFR	*Borrichia frutescens*	Sea ox-eye
DISP	*Distichlis spicata*	Saltgrass
ELEO	*Eleocharis spp.*	NA
FICA	*Fimbristylis castanea*	Marsh fimbry
HYBO	*Hydrocotyle bonariensis*	Largeleaf pennywort
ILVO	*Ilex vomitoria*	Yaupon holly
IMCY	*Imperata cylindrica*	Cogongrass
IPSA	*Ipomea sagittata*	Saltmarsh morning-glory
IVFR	*Iva frutescens*	Jesuit's bark
JURO	*Juncus roemerianus*	Black needlerush
LAPA	*Lathyrus palustris*	Marsh pea
LICA	*Lilaeopsis carolinensis*	Carolina grasswort
MYCE	*Myrica cerifera*	Southern wax myrtle
PADI	*Paspalum distichum*	Knotgrass
PARE	*Panicum repens*	Torpedo grass
PIEL	*Pinus elliottii*	Slash pine
QUE1	*Quercus spp. 1*	Aquatic oak
QUE2	*Quercus spp. 2*	Oak
RUTR	*Rubus trivialis*	Southern dewberry
SALA	*Sagittaria lancifolia*	Bull tongue arrowhead
SCAM	*Schoenoplectus americanus*	Chairmakers bulrush
SCRO	*Bolboschoenus robustus*	Sturdy bulrush
SMRO	*Smilax rotundifolia*	Roundleaf greenbrier
SOSE	*Solidago sempervirens*	Goldenrod
SPAL	*Sporobolus alterniflorus*	Smooth cordgrass
SPCY	*Spartina cynosuroides*	Big cordgrass
SPPA	*Spartina patens*	Saltmeadow cordgrass
SPSP	*Spartina spartinae*	Gulf cordgrass
SYTE	*Symphyotrichum tenuifolium*	Perennial saltmarsh American aster
TRPA	*Tripolium pannonicum*	Seashore aster
TRSE	*Triadica sebifera*	Chinese tallow tree
TURF	Unknown	Turf grass
UNK1	Unknown 1	NA
UNK2	Unknown 2	Weed
UNK3	Unknown 3	Purple vine

Appendix B

Analysis of wave gauge data

The significant wave period was statistically different among the six sites ($H_5 = 17.93, p < 0.00$). The significant wave period at AL ($M = 4.39$ s, $SE = 0.79$ s) was greater than at ST ($M = 2.73$ s, $SE = 0.08$ s), HC ($M = 2.72$ s, $SE = 0.29$ s), CW ($M = 2.06$ s, $SE = 0.20$ s), GB ($M = 1.67$ s, $SE = 0.46$ s), and OS ($M = 0.43$ s, $SE = 0.43$ s) (Fig. B1). Of the six sites, the only two that were significantly different from each other were AL and OS. The significant wave period was also significantly different between the high and low wave power (WP) groups ($H_1 = 13.11, p < 0.00$) with the high WP group ($M = 3.13$ s, $SE = 0.28$ s) greater than the low WP group ($M = 1.49$ s, $SE = 0.26$ s). The significant wave period is the wave period for the top one-third of the wave height. This indicated that the significant wave period is affected by the wave height.

The average wave height was significantly different among the six sites ($H_5 = 21.24, p < 0.00$) and the two WP groups ($H_1 = 18.16, p < 0.00$). Hancock County ($M = 0.08$ m, $SE = 0.01$ m) had the greatest average wave height of all six sites, followed by ST ($M = 0.07$ m, $SE = 0.01$ m), and AL ($M = 0.06$ m, $SE = 0.00$ m) which were not significantly different from each other (Fig B1). The lowest average wave height was at OS ($M = 0.03$ m, $SE = 0.01$ m) and was significantly different from HC, ST, and AL. Between the high and low averages were CW ($M = 0.05$ m, $SE = 0.00$ m) and GB ($M = 0.04$ m, $SE = 0.01$). The high WP group ($M = 0.07$ m, $SE = 0.00$ m) was greater than the low WP group ($M = 0.04$ m, $SE = 0.00$ m). The results from the average wave height data indicate that site shoreline orientation and available shoreline perpendicular fetch distance may influence the formation of wave height.

The maximum wave height was significantly different among the six sites ($H_5 = 22.97, p < 0.00$) and the two WP groups ($H_1 = 20.18, p < 0.00$). The maximum wave height was greatest at HC ($M = 0.39$ m, $SE = 0.09$ m), followed by ST ($M = 0.38$ m, $SE = 0.06$ m), AL ($M = 0.32$ m, $SE = 0.15$ m), CW ($M = 0.11$ m, $SE = 0.01$ m), GB ($M = 0.04$ m, $SE = 0.01$ m), and OS ($M = 0.03$ m, $SE = 0.01$ m) (Fig. B1). Statistical grouping for the maximum wave height grouped HC, ST, and AL together and CW, OS, and GB together. The maximum wave height for the high WP group ($M = 0.36$ m, $SE = 0.05$ m) was more than five times greater than the low WP group (M = 0.07 m, $SE = 0.01$ m).

Finally, the significant wave height was also significantly different among the six sites ($H_5 = 20.15, p < 0.00$) and the two WP groups ($H_1 = 17.05, p < 0.00$). The significant wave height is the average wave height for the top third of all wave heights. Hancock County ($M = 0.12$ m, $SE = 0.01$ m) had the greatest significant wave height and was significantly different from CW ($M = 0.06$ m, $SE = 0.00$ m), GB ($M = 0.04$ m, $SE = 0.01$ m), and OS ($M = 0.01$ m, $SE = 0.01$ m). Swift Tract ($M = 0.09$ m, $SE = 0.01$ m) and AL ($M = 0.09$ m, $SE = 0.01$ m) were between the two groups. The high WP group ($M = 0.10$ m, $SE = 0.01$ m) had more than double the significant wave height than the low WP group ($M = 0.04$ m, $SE = 0.01$). This finding indicates that the significant wave height may be influenced by the available fetch distance and wind power. The average wave height, significant wave height, significant wave period, and maximum wave height all decreased with average wave power (Fig B1). Shoreline type (NS, LS, HS) had no significant effect on any of these parameters.

The wave height percentiles show that the three high WP sites (HC, ST, and AL) have higher wave heights than the low WP sites (CW, OS, and GB) (Fig. B2). The jump between the 99th and 100th percentile is largest at ST (0.24 m), followed by HC (0.18 m), AL (0.16 m), CW (0.02 m), OS (0.004 m), and GB (0.004 m). The high WP group showed a jump between the 99th and 100th percentile of 0.19 m, which was almost 19 times greater than the low WP group (0.01 m) (Fig B2). This data is another way to represent the wave gauge data and show the difference between the six sites and how the wave energy may affect other factors in the water, such as turbidity.

Table B.1. Average wave power, significant wave period, average wave height, maximum wave height, and significant wave height for the high and low wave power groups.

Wave Power Group	Average Wave Power (kW/m)	Significant Wave Period (s)	Average Wave Height (m)	Maximum Wave Height (m)	Significant Wave Height (m)
High	6.91 ± 0.95	3.13 ± 0.28	0.07 ± 0.00	0.36 ± 0.05	0.10 ± 0.01
Low	1.31 ± 0.23	1.49 ± 0.26	0.04 ± 0.00	0.07 ± 0.01	0.04 ± 0.01

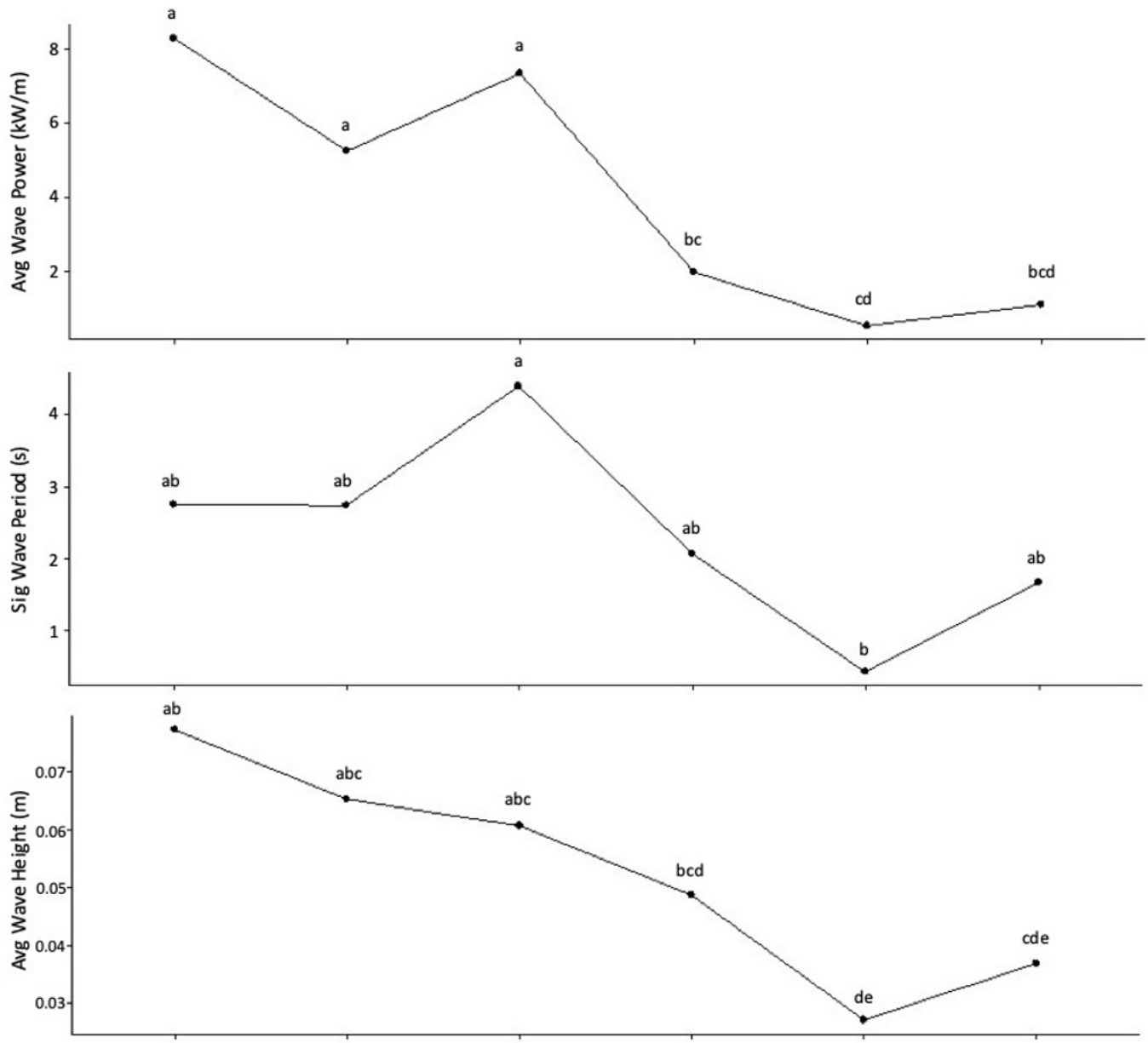

Figure B.1. Average wave power (kW/m), significant wave period (s), and average wave height (m) for the six sites. Significant differences by site are indicated by letter grouping based on the Wilcoxon Signed Rank Test.

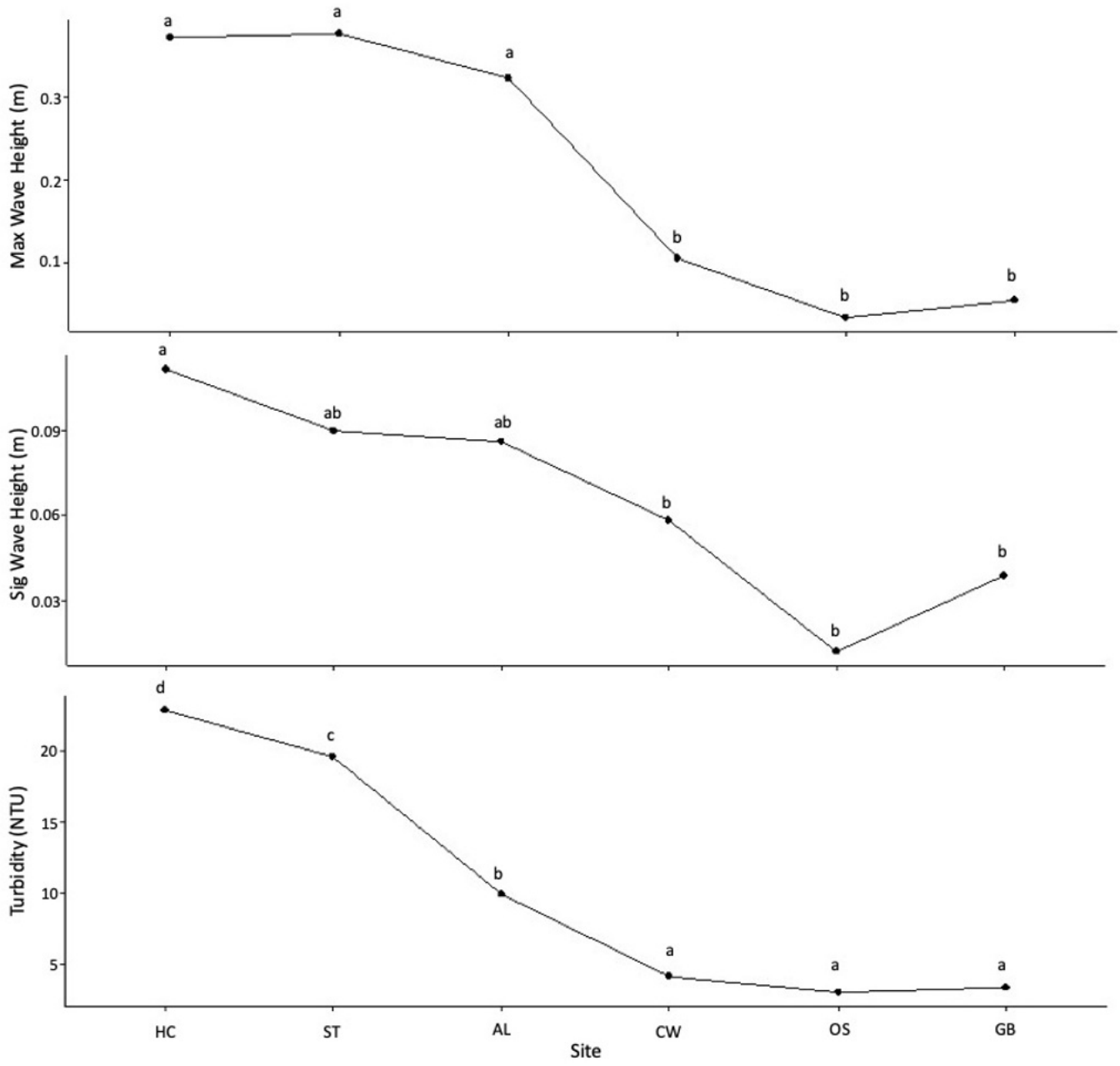

Figure B.1. cont'd. Maximum wave height (m), significant wave height (m), and turbidity (NTU) for the six sites. Significant differences by site are indicated by letter grouping based on the Wilcoxon Signed Rank Test.

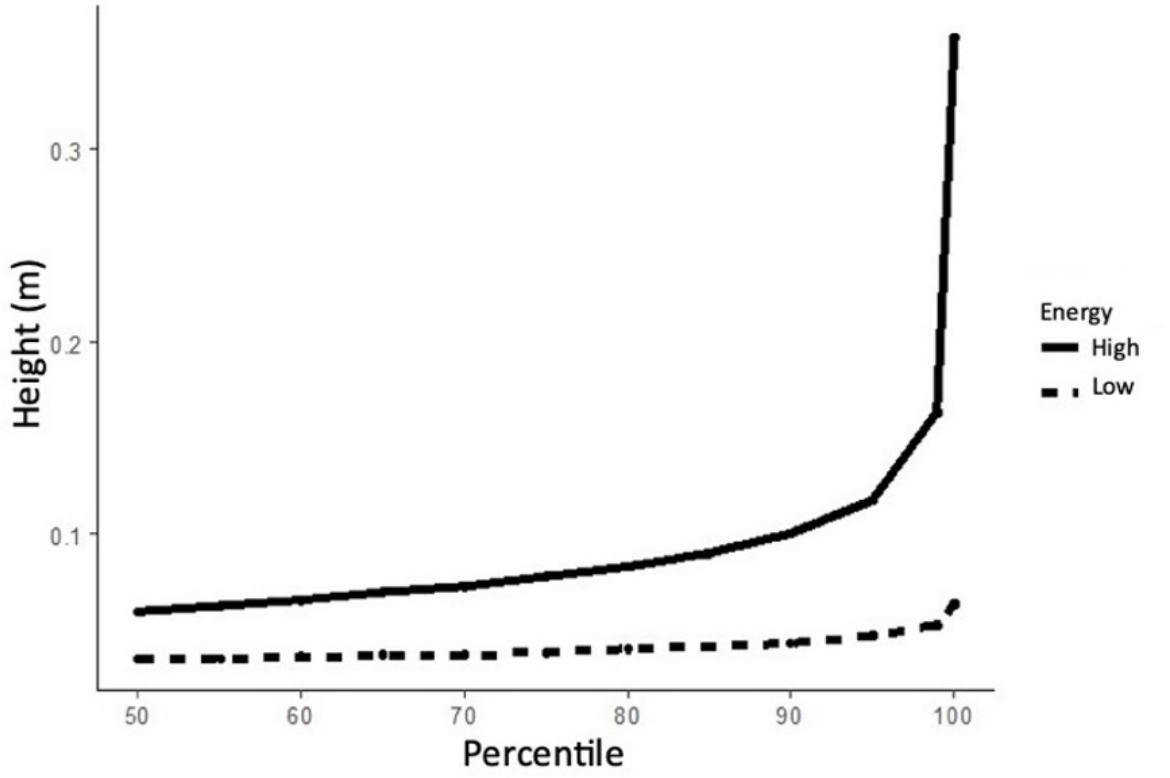

Figure B.2. Wave height percentiles from 50-100% showing the height (m) for high and low wave power groups.

References

- Álvarez-Rogel, J., del Carmen Tercero, M., Arce, M. I., Delgado, M. J., Conesa, H. M., & González-Alcaraz, M. N. (2016). Nitrate removal and potential soil N2O emissions in eutrophic salt marshes with and without Phragmites australis. *Geoderma*, *282*, 49–58. https://doi.org/10.1016/j.geoderma.2016.07.011
- Arkema, K. K., Guannel, G., Verutes, G., Wood, S. A., Guerry, A., Ruckelshaus, M., Kareiva, P., Lacayo, M., & Silver, J. M. (2013). Coastal habitats shield people and property from sea-level rise and storms. *Nature Climate Change*, *3*(10), 913–918. https://doi.org/10.1038/nclimate1944
- Augustin, L. N., Irish, J. L., & Lynett, P. (2009). Laboratory and numerical studies of wave damping by emergent and near-emergent wetland vegetation. *Coastal Engineering*, *56*(3), 332–340. https://doi.org/10.1016/j.coastaleng.2008.09.004
- Balouskus, R. G., & Targett, T. E. (2016). Fish and Blue Crab Density along a Riprap-Sill-Hardened Shoreline: Comparisons with Spartina Marsh and Riprap. *Transactions of the American Fisheries Society*, *145*(4), 766–773. https://doi.org/10.1080/00028487.2016.1172508
- Basco, D. R. (2006). Seawall Impacts on Adjacent Beaches : Separating Fact from Fiction.*Journal of Coastal Research*, *II*(39), 741–744.
- Bayraktarov, E., Saunders, M. I., Abdullah, S., Mills, M., Beher, J., Possingham, H. P., Mumby, P. J., & Lovelock, C. E. (2015). The cost and feasibility of marine coastal restoration. *Ecological Applications*, *26*(4), 1055–1074.

https://doi.org/10.1890/15-1077.1

- Bilkovic, D. M., & Mitchell, M. M. (2013). Ecological tradeoffs of stabilized salt marshes as a shoreline protection strategy: Effects of artificial structures on macrobenthic assemblages. *Ecological Engineering*, *61*, 469–481. https://doi.org/10.1016/j.ecoleng.2013.10.011
- Bilkovic, D. M., & Roggero, M. M. (2008). Effects of coastal development on nearshore estuarine nekton communities. *Marine Ecology Progress Series*, *358*, 27–39. https://doi.org/10.3354/meps07279
- Bilkovic, D. M., & Mitchell, M. M. (2018). Designing Living Shoreline Salt Marsh Ecosystems to Promote Coastal Resilience. *Living Shorelines*, *April*, 293–316. https://doi.org/10.1201/9781315151465-19
- Bilkovic, D. M., Mitchell, M., Mason, P., & Duhring, K. (2016). The Role of Living Shorelines as Estuarine Habitat Conservation Strategies. *Coastal Management*, *44*(3), 161–174. https://doi.org/10.1080/08920753.2016.1160201
- Boerema, A., Geerts, L., Oosterlee, L., Temmerman, S., & Meire, P. (2016). Ecosystem service delivery in restoration projects: The effect of ecological succession on the benefits of tidal marsh restoration. *Ecology and Society*, *21*(2). https://doi.org/10.5751/ES-08372-210210
- Bozek, C. M., & Burdick, D. M. (2005). Impacts of seawalls on saltmarsh plant communities in the Great Bay Estuary, New Hampshire USA. *Wetlands Ecology and Management*, *13*(5), 553–568. https://doi.org/10.1007/s11273-004-5543-z
- Brueske, C. C., & Barrett, G. W. (1994). Effects of vegetation and hydrologic load on sedimentation patterns in experimental wetland ecosystems. *Ecological Engineering*, *3*(4), 429–447. https://doi.org/10.1016/0925-8574(94)00011-5
- Cattrijsse, A., Dankwa, H. R., & Mees, J. (1997). Nursery function of an estuarine tidal marsh for the brown shrimp Crangon crangon. *Journal of Sea Research*, *38*(1–2), 109–121. https://doi.org/10.1016/S1385-1101(97)00036-1
- Clewell, A. (1985). Guide to the vascular plants of the Florida panhandle. Florida State University Press, University Presses of Florida.
- Correll, D., Johnston, M. (1970). Manual of the vascular plants of Texas. Texas Research Foundation.
- Craft, C., Clough, J., Ehman, J., Jove, S., Park, R., Pennings, S., Guo, H., & Machmuller, M. (2009). Forecasting the effects of accelerated sea-level rise on tidal marsh ecosystem services. *Frontiers in Ecology and the Environment*, *7*(2), 73–78. https://doi.org/10.1890/070219
- Craft, C., Megonigal, P., Broome, S., Stevenson, J., Freese, R., Cornell, J., Zheng, L., & Sacco, J. (2003). The pace of ecosystem development of constructed Spartina alterniflora marshes. *Ecological Applications*, *13*(5), 1417–1432. https://doi.org/10.1890/02-5086
- Crum, K. P., Balouskus, R. G., & Targett, T. E. (2018). Growth and Movements of Mummichogs (Fundulus heteroclitus) Along Armored and Vegetated Estuarine Shorelines. *Estuaries and Coasts*, *41*(2018), 131–143. https://doi.org/10.1007/s12237-017-0299-x
- Currin, C. A., Delano, P. C., & Valdes-Weaver, L. M. (2008). Utilization of a citizen monitoring protocol to assess the structure and function of natural and stabilized fringing salt marshes in North Carolina. *Wetlands Ecology and Management*, *16*(2), 97–118. https://doi.org/10.1007/s11273-007-9059-1
- Davis, J. L., Currin, C. A., O'Brien, C., Raffenburg, C., & Davis, A. (2015). Living shorelines: Coastal resilience with a

blue carbon benefit. *PLoS ONE*, *10*(11), 1–18. https://doi.org/10.1371/journal.pone.0142595

- Doody, J. P. (2004). “Coastal squeeze” - An historical perspective. *Journal of Coastal Conservation*, *10*(1–2), 129–138. https://doi.org/10.1652/1400-0350(2004)010[0129:CSAHP]2.0.CO;2
- Duhring, K. A, Barnard, T. A, & Hardaway, S. (2006). *A survey of the effectiveness of existing marsh toe protection structures in Virginia*. *July*.
- Eleuterius, L. (1972). The marshes of Mississippi. *Castanea*, *37*(3), 153–168. http://www.jstor.org/stable/4032384
- Erdle, S., Davis, J., & Sellner, K. (2006). Management, Policy, Science, and Engineering of Nonstructural Erosion Control in the Chesapeake Bay. *Proceedings of the 2006 Living Shoreline Summit.*
- Feagin, R. A., Lozada-Bernard, S. M., Ravens, T. M., Möller, I., Yeager, K. M., & Baird, A. H. (2009). Does vegetation prevent wave erosion of salt marsh edges? *Proceedings of the National Academy of Sciences of the United States of America*, *106*(25), 10109–10113. https://doi.org/10.1073/pnas.0901297106
- Fonseca, M. S., & Cahalan, J. A. (1992). A preliminary evaluation of wave attenuation by four species of seagrass. *Estuarine, Coastal and Shelf Science*, *35*(6), 565–576. https://doi.org/10.1016/S0272-7714(05)80039-3
- Gedan, K. B., Kirwan, M. L., Wolanski, E., Barbier, E. B., & Silliman, B. R. (2011). The present and future role of coastal wetland vegetation in protecting shorelines: Answering recent challenges to the paradigm. *Climatic Change*, *106*(1), 7–29. https://doi.org/10.1007/s10584-010-0003-7
- Gittman, R. K., Fodrie, F. J., Popowich, A. M., Keller, D. A., Bruno, J. F., Currin, C. A., Peterson, C. H., & Piehler, M. F. (2015). Engineering away our natural defenses: An analysis of shoreline hardening in the US. *Frontiers in Ecology and the Environment*, *13*(6), 301–307. https://doi.org/10.1890/150065
- Gittman, R. K., Scyphers, S. B., Smith, C. S., Neylan, I. P., & Grabowski, J. H. (2016). Ecological consequences of shoreline hardening: A meta-analysis. *BioScience*, *66*(9), 763–773. https://doi.org/10.1093/biosci/biw091
- Green, B. C., Smith, D. J., & Underwood, G. J. C. (2012). Habitat connectivity and spatial complexity differentially affect mangrove and salt marsh fish assemblages. *Marine Ecology Progress Series*, *466*, 177–192. https://doi.org/10.3354/meps09791
- Herbert, D., Astrom, E., Bersoza, A. C., Batzer, A., McGovern, P., Angelini, C., Wasman, S., Dix, N., & Sheremet, A. (2018). Mitigating erosional effects induced by boat wakes with living shorelines. *Sustainability (Switzerland)*, *10*(2), 1–19. https://doi.org/10.3390/su10020436
- Himmelstoss, E.A., R. E. Henderson, M. G. Kratzmann, A. S. Farris. (2021). Digital Shoreline Analysis System (DSAS) user guide. Coastal and Marine Hazards and Resources Program, Woods Hole Coastal and Marine Science Center, doi/ 10.3133/ofr20211091
- IPCC, 2021: Climate Change 2021: The Physical Science Basis. Contribution of Working Group I to the Sixth Assessment Report of the Intergovernmental Panel on Climate Change[Masson-Delmotte, V., P. Zhai, A. Pirani, S.L. Connors, C. Péan, S. Berger, N. Caud, Y. Chen, L. Goldfarb, M.I. Gomis, M. Huang, K. Leitzell, E. Lonnoy, J.B.R. Matthews, T.K. Maycock, T. Waterfield, O. Yelekçi, R. Yu, and B. Zhou (eds.)]. Cambridge University Press, Cambridge, United Kingdom and New York, NY, USA, In press, doi:10.1017/9781009157896.
- Johnson, D. S., Warren, R. S., Deegan, L. A., & Mozdzer, T. J. (2016). Saltmarsh plant responses to eutrophication. *Ecological Applications*, *26*(8), 2647–2659. https://doi.org/10.1002/eap.1402

- Juneau, Brittany. 2021. Differences in Erosion Rates and Elevation Among Natural, Living and Hardened Shorelines in Mississippi, and Alabama. Honor's thesis. Department of Coastal Sciences, The University of Southern Mississippi
- La Peyre, M. K., Humphries, A. T., Casas, S. M., & La Peyre, J. F. (2014). Temporal variation in development of ecosystem services from oyster reef restoration. *Ecological Engineering*, *63*, 34–44. https://doi.org/10.1016/j.ecoleng.2013.12.001
- Leonardi, N., Ganju, N. K., & Fagherazzi, S. (2016). A linear relationship between wave power and erosion determines salt-marsh resilience to violent storms and hurricanes. *Proceedings of the National Academy of Sciences*, *113*(1), 64–68. https://doi.org/10.1073/pnas.1510095112
- Madsen, J. D., Chambers, P. A., James, W. F., Koch, E. W., & Westlake, D. F. (2001). The interaction between water movement, sediment dynamics and submersed macrophytes. *Hydrobiologia*, *444*, 71–84. https://doi.org/10.1023/A:1017520800568
- Matzke, S., & Elsey-Quirk, T. (2018). *Spartina Patens* Productivity and Soil Organic Matter Response to Sedimentation and Nutrient Enrichment. *Wetlands*, *38*(6), 1233–1244. https://doi.org/10.1007/s13157-018-1030-9
- Mitchell, M., & Bilkovic, D. M. (2019). Embracing dynamic design for climate-resilient living shorelines. *Journal of Applied Ecology*, *56*(5), 1099–1105. https://doi.org/10.1111/1365-2664.13371
- Molinaroli, E., Guerzoni, S., De Falco, G., Sarretta, A., Cucco, A., Como, S., Simeone, S., Perilli, A., & Magni, P. (2009). Relationships between hydrodynamic parameters and grain size in two contrasting transitional environments: The Lagoons of Venice and Cabras, Italy. *Sedimentary Geology*, *219*(1–4), 196–207. https://doi.org/10.1016/j.sedgeo.2009.05.013
- Nelson, P. A. (2008). Ecological effects of wave energy conversion technology on California's marine and anadromous fishes. *Developing Wave Energy in Coastal California: Potential Socio-Economic and Environmental Effects*, *November*, 111–135. http://www.energy.ca.gov/2008publications/CEC-500-2008-083/CEC-500-2008-083.PDF
- NOAA 2013a. Hancock County Marsh Living Shoreline Project https://www.gulfspillrestoration.noaa.gov/wp-content/uploads/Living_ShoreFINAL12_1_13.pdf
- NOAA 2013b. Swift Tract Living Shoreline Project https://www.gulfspillrestoration.noaa.gov/wp-content/uploads/SwiftTract_FINAL12_2_13.pdf
- NOAA 2016. Planning for Future Flood Hazards in Mississippi https://coast.noaa.gov/digitalcoast/stories/ocean-springs.html
- O'Donnell, J. E. D. (2017). Living Shorelines: A Review of Literature Relevant to New England Coasts. *Journal of Coastal Research*, *332*(2), 435–451. https://doi.org/10.2112/jcoastres-d-15-00184.1
- Oksanen, J., F.G. Blanchett, M. Friendly et al. 2020. Community Ecology Package ver. 2.5. Available at https://cran.r-project.org/web/packages/vegan/vegan.pdf
- Palinkas, C. M., Sanford, L. P., & Koch, E. W. (2018). Influence of Shoreline Stabilization Structures on the Nearshore Sedimentary Environment in Mesohaline Chesapeake Bay. *Estuaries and Coasts*, *41*(4), 952–965. https://doi.org/10.1007/s12237-017-0339-6
- Partyka, M. L., Peterson, M. S., Partyka, M. L., & Peterson, M. S. (2017). Habitat Quality and Salt-Marsh Species Assemblages along an Anthropogenic Estuarine Landscape. *Journal Coastal Research* 24(6), 1570–1581

http://www.jstor.org/stable/40065141

- Pennings, S. C., Grant, M. B., & Bertness, M. D. (2005). Plant zonation in low-latitude salt marshes: Disentangling the roles of flooding, salinity and competition. *Journal of Ecology*, *93*(1), 159–167. https://doi.org/10.1111/j.1365-2745.2004.00959.x
- Polk, M. A., & Eulie, D. O. (2018). Effectiveness of Living Shorelines as an Erosion Control Method in North Carolina. *Estuaries and Coasts*, *41*(8), 2212–2222. https://doi.org/10.1007/s12237-018-0439-y
- Radford A, Ahles H, Bell C (1983) Manual of the vascular flora of the Carolinas. University of North Carolina Press
- Roberts, S. (2010). A report from the National Research Council—Mitigating shore erosion along sheltered coasts. *Shipman, H., Dethier, MN, Gelfenbaum, G., Fresh, KL, and Dinicola, RS, Eds, January 2010*, 85–90.
- Ruggiero, P. (2009). Impacts of shoreline armoring on sediment dynamics.*Puget Sound Shorelines and the Impacts of Armoring—Proceedings of a State of the Science Workshop*, *February 2015*, 179–186.
- Scyphers, S. B., Powers, S. P., Heck, K. L., & Byron, D. (2011). Oyster reefs as natural breakwaters mitigate shoreline loss and facilitate fisheries. *PLoS ONE*, *6*(8). https://doi.org/10.1371/journal.pone.0022396
- Sicangco, C., Collini, R., Martin, S., Monti, A., Sparks, E. (2021). Cost-benefit analysis of a small-scale living shoreline project https://repository.library.noaa.gov/view/noaa/48521
- Silliman, B. R., He, Q., Angelini, C., Smith, C. S., Kirwan, M. L., Daleo, P., Renzi, J. J., Butler, J., Osborne, T. Z., Nifong, J. C., & van de Koppel, J. (2019). Field Experiments and Meta-analysis Reveal Wetland Vegetation as a Crucial Element in the Coastal Protection Paradigm. *Current Biology*, *29*(11), 1800-1806.e3. https://doi.org/10.1016/j.cub.2019.05.017
- Sparks, E. L., Cebrian, J., Biber, P. D., Sheehan, K. L., & Tobias, C. R. (2013). Cost-effectiveness of two small-scale salt marsh restoration designs. *Ecological Engineering*, *53*, 250–256. https://doi.org/10.1016/j.ecoleng.2012.12.053
- Spellmann, G., "A Comparison of Natural, Living, and Hardened Shorelines Ability to Prevent Coastal Erosion and Maintain a Healthy Ecosystem" (2022). *Master's Theses*. 904. https://aquila.usm.edu/masters_theses/904
- Sutton-Grier, A. E., Wowk, K., & Bamford, H. (2015). Future of our coasts: The potential for natural and hybrid infrastructure to enhance the resilience of our coastal communities, economies and ecosystems. *Environmental Science and Policy*, *51*, 137–148. https://doi.org/10.1016/j.envsci.2015.04.006
- Swann, L. (2008). The Use of Living Shorelines to Mitigate the Effects of Storm Events on Dauphin Island, Alabama, USA. *American Fisheries Society Symposium*, *64*.
- Sweet, W.V., Kopp, R.E., Weaver, C.P., Obeysekera, J., Horton, R.M., Thieler, E.R., Zervas, C. (2017). Global And Regional Sea Level Rise Scenarios For The United States. NOAA Technical Report NOS CO-OPS 083. https://tidesandcurrents.noaa.gov/publications/techrpt83_Global_and_Regional_SLR_Scenarios_for_the_US_final.pdf
- Temmerman, S., Meire, P., Bouma, T. J., Herman, P. M. J., Ysebaert, T., & De Vriend, H. J. (2013). Ecosystem-based coastal defence in the face of global change. *Nature*, *504*(7478), 79–83. https://doi.org/10.1038/nature12859
- Temple, N. A., Sparks, E. L., Webb, B. M., Cebrian, J., Virden, M. F., Lucore, A. E., & Moss, H. B. (2021). Responses of two fringing salt marsh plant species along a wave climate gradient. *Marine Ecology Progress Series*, *675*, 53–66. https://doi.org/10.3354/meps13843
- Valiela, I., & Cole, M. L. (2002). Comparative evidence that salt marshes and mangroves may protect seagrass

meadows from land-derived nitrogen loads. *Ecosystems*, *5*(1), 92–102. https://doi.org/10.1007/s10021-001-0058-4

- Vargas-Luna, A., Crosato, A., & Uijttewaal, W. S. J. (2015). Effects of vegetation on flow and sediment transport: Comparative analyses and validation of predicting models. *Earth Surface Processes and Landforms*, *40*(2), 157–176. https://doi.org/10.1002/esp.3633
- Vymazal, J. (2013). Emergent plants used in free water surface constructed wetlands: A review.*Ecological Engineering*, *61*, 582–592. https://doi.org/10.1016/j.ecoleng.2013.06.023
- Wu, W., Zhang, M., Ozeren, Y., & Wren, D. (2012). Analysis of Vegetation Effect on Waves Using a Vertical 2D RANS Model. *Journal of Coastal Research*, *287*(May), 383–397. https://doi.org/10.2112/jcoastres-d-12-00023.1